Seafloor geomorphology and glacimarine sedimentation associated with fast-flowing ice sheet outlet glaciers in Disko Bay, West Greenland

Katharina Streuff[a,*], Colm Ó Cofaigh[a], Kelly Hogan[b], Anne Jennings[c], Jeremy Lloyd[a], Riko Noormets[d], Tove Nielsen[e], Antoon Kuijpers[e], Julian A. Dowdeswell[f], Wilhelm Weinrebe[g]

[a]*Durham University, Department of Geography, South Road, Durham DH1 3LE, United Kingdom*
[b]*British Antarctic Survey, Natural Environmental Research Council, High Cross, Madingley Road, Cambridge, CB3 0ET, United Kingdom*
[c]*INSTAAR and Department of Geological Sciences, University of Colorado, Boulder, CO 80309-0450, USA*
[d]*The University Centre in Svalbard (UNIS), P.O. Box 156, N-9171 Longyearbyen, Norway*
[e]*Geological Survey of Denmark and Greenland, Øster Voldgade 10, 1350 Copenhagen, Denmark*
[f]*Scott Polar Research Institute, University of Cambridge, Lensfield Road, Cambridge, CB2 1ER, United Kingdom*
[g]*GEOMAR Helmholtz Centre for Ocean Research Kiel, Wischhofstr. 1-3, 24148 Kiel, Germany*

Abstract

Fast-flowing outlet glaciers currently drain the Greenland Ice Sheet (GIS), delivering ice, meltwater and debris to the fjords around Greenland. Although such glaciers strongly affect the ice sheet's mass balance, their glacimarine processes and associated products are still poorly understood. This study provides a detailed analysis of lithological and geophysical data from Disko Bay and the Vaigat Strait in central West Greenland. Disko Bay is strongly influenced by Jakobshavn Isbræ, Greenland's fastest-flowing glacier, which currently drains ~7% of the ice sheet. Streamlined glacial landforms record the former flow of an expanded Jakobshavn Isbræ and adjacent GIS outlets through Disko Bay

*Corresponding author
Email addresses: katharina.streuff@durham.ac.uk (Katharina Streuff), colm.ocofaigh@durham.ac.uk (Colm Ó Cofaigh), kelgan@bas.ac.uk (Kelly Hogan), anne.jennings@colorado.edu (Anne Jennings), j.m.lloyd@durham.ac.uk (Jeremy Lloyd), riko.noormets@unis.no (Riko Noormets), tni@geus.dk (Tove Nielsen), aku@geus.dk (Antoon Kuijpers), jd16@cam.ac.uk (Julian A. Dowdeswell), wweinrebe@geomar.de (Wilhelm Weinrebe)

and the Vaigat Strait towards the continental shelf. Thirteen vibrocores contain a complex set of lithofacies including diamict, stratified mud, interbedded mud and sand, and bioturbated mud deposited by (1) suspension settling from meltwater plumes and the water column, (2) sediment gravity flows, and (3) iceberg rafting and ploughing. The importance of meltwater-related processes to glacimarine sedimentation in West Greenland fjords and bays is emphasised by the abundance of mud preserved in the cores. Radiocarbon dates constrain the position of the ice margin during deglaciation, and suggest that Jakobshavn Isbræ had retreated into central Disko Bay before 10.6 cal ka BP and to beyond Isfjeldsbanken by 7.6–7.1 cal ka BP. Sediment accumulation rates were up to 1.7 cm a^{-1} for ice-proximal glacimarine mud, and $\sim$0.007–0.05 cm a^{-1} for overlying distal sediments. In addition to elucidating the deglacial retreat history of Jakobshavn Isbræ, our findings show that the glacimarine sedimentary processes in West Greenland are similar to those in East Greenland, and that variability in such processes is more a function of time and glacier proximity than of geographic location and associated climatic regime.

Keywords: Glacial geomorphology, sedimentology, Holocene, Greenland, deglaciation, tidewater glaciers

---

1. Introduction

Tidewater glaciers terminate in the ocean at a grounded ice front (Meier & Post, 1987), represent an important link between terrestrial and marine environments, and are particularly susceptible to climate change. Along the coast of Greenland many fast-flowing outlet glaciers drain the interior of the Greenland Ice Sheet (GIS), terminating as tidewater margins in the surrounding fjords. The associated glacial landforms and glacimarine sediments are revealed as the glaciers retreat, and provide important archives for understanding the long-term glacial evolution of the ice sheet and its future role with respect to sea-level rise (cf. e.g. Alley et al., 2005; Bamber et al., 2007; Nick et al., 2009; Ó Cofaigh et al., 2013; Dowdeswell et al., 2014; Lane et al., 2014; Joughin et al., 2014;

Hogan et al., 2016; Sheldon et al., 2016). Jakobshavn Isbræ, in central West Greenland, is of particular interest in this context, as it is the fastest-flowing of these outlets, currently flowing at velocities >17 km a^{-1} and draining ~7% of the GIS, and thus exerts a strong influence on the ice sheet's mass balance (e.g. Bindschadler, 1984; Joughin et al., 2004; Rignot & Kanagaratnam, 2006; Joughin et al., 2014). Indeed, the increasing retreat speed and break-up of the glacier tongue has led to a rise in global sea level of almost 1 mm between 2000 and 2011 (Howat et al., 2011; Joughin et al., 2014). Although a number of investigations have focussed on the short-term dynamics of GIS outlet glaciers (e.g. Joughin et al., 2004; Moon & Joughin, 2008; Joughin et al., 2014), knowledge about their longer-term flow dynamics, their glacimarine processes, and the overall interaction of the glaciers with the marine environment since the Last Glacial Maximum (LGM) is only just emerging (e.g. Long & Roberts, 2003; Young et al., 2011a; Jennings et al., 2013; Ó Cofaigh et al., 2013; Dowdeswell et al., 2014; Hogan et al., 2016; Sheldon et al., 2016). This study uses sediment cores, multibeam bathymetry, sub-bottom profiler data, and radiocarbon dates from Disko Bay and the Vaigat Strait (Fig. 1) to (1) investigate the Holocene glacimarine sedimentary processes and products in Disko Bay and (2) to elucidate the deglacial history of Jakobshavn Isbræ in order to see how this particular outlet responded to environmental changes since the LGM.

2. Study area

2.1. Physiographic setting

Disko Bay is a marine embayment in central West Greenland, which is separated from the Vaigat Strait, a relatively narrow deep water trough, by Disko Island (Fig. 1). Disko Bay is located between ~68°30'–69°40'N and 50°50'–55°00'W, and is roughly 100 km wide and between 50 and 500 m deep. It covers an area of ~18000 km^2 and is bounded by Isfjorden and the Greenland mainland to the east, and Baffin Bay to the west (Fig. 1). A large, relatively shallow ridge,

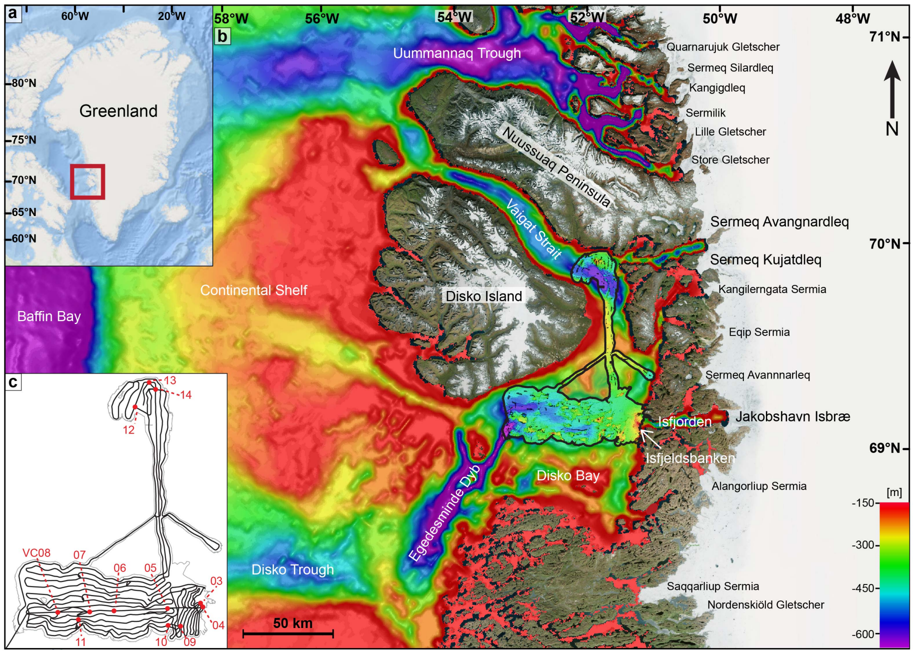

Figure 1: a) Overview of Greenland with red rectangle indicating the extent of b). b) Study area and local bathymetry (IBCAO). The black outline shows the extent of the bathymetric data available for this study. Purple areas indicate bathymetric troughs. c) Distribution of TOPAS lines and location of the vibrocores.

Isfjeldsbanken, is located at the entrance of the smaller Isfjorden and serves as a sill between the latter and Disko Bay. The Vaigat Strait is situated between $\sim$69°40'– 70°50'N and 50°50'-55°00'W (Fig. 1), is 10–30 km wide, and 200–650 m deep. It is bounded by the Nuussuaq Peninsula to the north and east and Disko Island to the south and west (Fig. 1). Three larger basins are present in the study area, one in the Vaigat Strait (up to 650 m deep) and two in western Disko Bay. The latter are $\sim$800 m deep and part of Egedesminde Dyb, a large trough, which is orientated northeast-southwest linking Disko Bay with the continental shelf (Fig. 1b). The local geology is dominated by Precambrian basement, including crystalline rocks such as granites and orthogneisses along the western shore of the Greenland mainland, Palaeogene basalts on Disko Island and western Nuussuaq, and Palaeogene and Upper Cretaceous sediments exposed at the seafloor and on parts of Disko Island and the Nuussuaq Peninsula (Chalmers et al., 1999; Larsen & Pulvertaft, 2000; Weidick & Bennike, 2007).

2.2. Glacial background

Although there are still gaps in our understanding of the long-term evolution of the GIS and its outlet glaciers (cf. Funder et al., 2011), recent studies have outlined the Pliocene-Pleistocene glacial development of the Disko Bay margin (Hofmann et al., 2016), and established that during the LGM an extended Jakobshavn Isbræ and several other glaciers in the area drained the GIS via Disko Bay and the Vaigat Strait, and extended to the outer shelf edge (Ó Cofaigh et al., 2013; Jennings et al., 2013; Hogan et al., 2016). Radiocarbon dates from reworked shells from the Disko trough-mouth fan and tills on the adjoining shelf suggest that retreat of Jakobshavn Isbræ was underway by at least 13.8 ka BP and was briefly interrupted around 12.3–12 ka BP when the ice sheet underwent a re-advance in Disko Trough during the Younger Dryas (Ó Cofaigh et al., 2013). Two modes of ice retreat have been suggested, (1) fast and relatively continuous retreat from the continental shelf and through Disko Bay (e.g. Long & Roberts, 2003; Lloyd et al., 2005; Hogan et al., 2012; Kelley et al., 2013), and (2) step-wise retreat, where Jakobshavn Isbræ experienced short periods of still-stand at bedrock highs (e.g. Weidick, 1996; Rasch, 2000; Hogan et al., 2016). This led to the general consensus that retreat across the continental shelf and through Disko Bay was relatively fast, but slowed once the ice stream entered Isfjorden in the east (cf. Funder & Hansen, 1996; Lloyd et al., 2005; Hogan et al., 2012; Kelley et al., 2013; Ó Cofaigh et al., 2013).

Deglaciation of western Disko Bay commenced around 10.8 ka BP, and the bay's eastern part was ice-free by 10.2 ka BP (Lloyd et al., 2005; Kelley et al., 2013). The grounded margin of Jakobshavn Isbræ most likely reached Isfjeldsbanken in eastern Disko Bay around 10.1 ka BP, pausing there until ∼7.9 ka BP, when it retreated into Isfjorden (see Fig. 1b; Lloyd et al., 2005; Weidick & Bennike, 2007; Kelley et al., 2013). At present the Jakobshavn Isbræ margin is located approximately 50 km east of Isfjeldsbanken and discharges 90–100 km^3 a^{-1} of ice into Isfjorden (Joughin et al., 2014). Due to a shorter calving line, the calving flux from Jakobshavn Isbræ was suggested to be significantly reduced around 9-10 ka BP, when the glacier margin was at Isfjeldsbanken, and the glaciers in northeast Disko Bay were inferred to be the dominant source of ice-rafted debris (IRD) during this time (Weidick, 1994; Long & Roberts, 2003; McCarthy, 2011). Retreat of the outer parts of the GIS outlets was asynchronous along Greenland's western coast (Ó Cofaigh et al., 2013; Sheldon et al., 2016), and deglaciation in the Vaigat was underway by 12.4 ka BP, with its western part ice-free before 11.8 ka BP and its eastern part deglaciated before 10.0 ka BP (Weidick, 1968; Bennike, 2000).

2.3. Oceanography

During deglaciation and the early Holocene, ocean waters in Disko Bay and the Vaigat Strait were mainly dominated by cold and fresh meltwater from the GIS (e.g. Lloyd et al., 2005; Jennings et al., 2013). By approximately 10 ka BP, the West Greenland Current (WGC) started to bring warmer and more saline waters into the bay, influencing the coastal areas around 7.8 ka BP, when ice had retreated into Isfjorden and the meltwater flux into Disko Bay had decreased (Lloyd et al., 2005; Lloyd, 2006). After c. 6 ka BP the regional circulation pattern started to resemble modern conditions (Perner et al., 2013), and today the modern tidewater glaciers still influence the surface waters in Disko Bay and the Vaigat Strait, which are cold and fresh (Andersen, 1981; Ribergaard & Buch, 2008). The bottom waters, however, contain warmer and more saline waters from the WGC (Lloyd et al., 2005; Perner et al., 2013). These waters are advected through Disko Bay from west to east and flow northwards around Disko Island and through the Vaigat Strait (e.g. Andresen et al., 2010). They not only influence iceberg calving rates, but have also been linked to increased thinning and melting of GIS outlet glaciers (Holland et al., 2008; Rignot et al., 2010; Kelley et al., 2013).

2.4. Acoustic stratigraphy of marine sediments

The sub-bottom profiler data available for this study were previously described and interpreted by Hogan et al. (2011, 2012), who identified four acoustic facies in Disko Bay, AD1–AD4, culminating in a total maximum thickness of up to 258 $\pm$ 8 m (calculated using a p-wave velocity of 1610 m s^{-1}; Fig. 2a, b). Facies AD1, with a stratified acoustic signature and a strong upper reflection (Fig. 2a), is 16–64 m thick, has onlap-fill geometry, and forms wedges in places (Hogan et al., 2012). Facies AD2 generally overlies and locally cuts into AD1, is composed of acoustically transparent sub-units, and shows tapered or wedge-shaped geometry. It is 4–32 m thick and its upper boundary generally occurs as a continuous reflection of high amplitude (Fig. 2a; Hogan et al., 2012). Facies AD3, like AD1, is acoustically stratified with internal reflections of medium strength (Fig. 2a). AD3 conformably overlies AD2, drapes some of the bedrock highs in the area and is up to 13 m thick. Facies AD4 only occurs in parts of Disko Bay, where it appears acoustically transparent with weak and chaotic internal reflections protruding into AD1 and AD2, and a strong, hummocky and chaotic upper boundary (Fig. 2a; Hogan et al., 2012).

In southern Vaigat, Hogan et al. (2012) distinguished a total of five acoustic facies, AV1-AV5, with a cumulative thickness of up to 109 $\pm$ 3 m (Fig. 2c, d). Facies AV1, AV2, AV3, and AV4 are acoustically homogeneous with generally weak, discontinuous to chaotic internal reflections and are bounded by medium-strong, mostly continuous upper, in places hummocky, reflections. A distinction into four acoustic facies was mostly based on different morphologies; while AV1 represents the deepest basin-infill strata in the Vaigat, AV2 has a distinct wedge-shape, AV3 occurs as lenticular bodies, and AV4 infills surface depressions of AV2 and AV3 (Fig. 2c, d).

Facies AD1 was inferred to contain sediment deposited from turbid meltwater plumes, from the water column, icebergs, and sediment gravity flows in an ice-proximal environment in the eastern bay and in an ice-distal environment in the western bay (Hogan et al., 2011, 2012). From the tapered/wedge-shaped

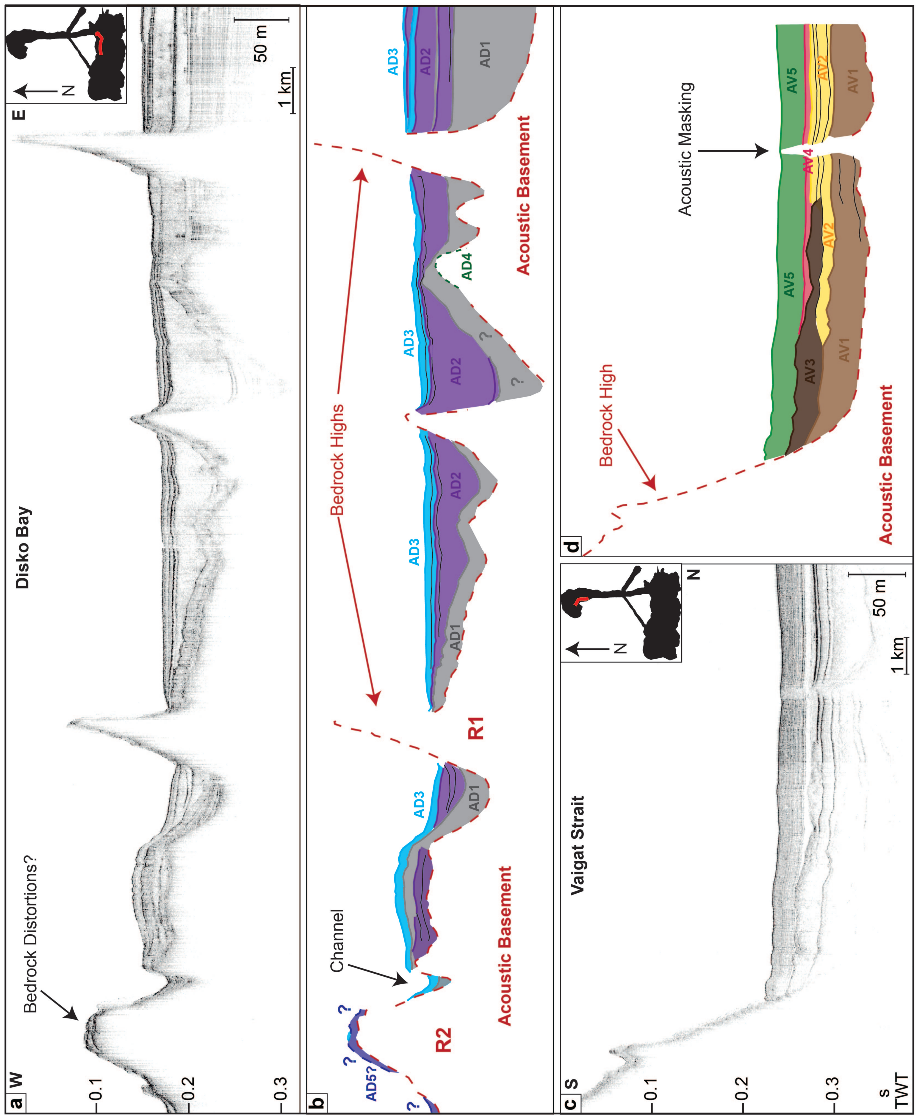

Figure 2: a) TOPAS profile showing an example of the acoustic facies in Disko Bay. b) Interpretation of acoustic facies in Disko Bay, after Hogan et al. (2012). c) TOPAS profile with examples of acoustic facies occurring in the Vaigat Strait. d) Acoustic facies interpretation in the Vaigat Strait based on Hogan et al. (2012). The red lines on the black polygons indicate the respective location of the profiles.

geometry and the acoustic transparency, the sub-units of AD2 were interpreted to also reflect gravity-flow deposits. These are occasionally interbedded with thin sediment strata derived from hemipelagic sedimentation, bottom currents, and smaller-scale or more dilute gravity flows (Hogan et al., 2012). Hogan et al. (2011, 2012) interpreted Facies AD3 as ice-distal sediments settling from hemipelagic sedimentation and icebergs and/or sea ice. The internal reflections were associated with variations in input of IRD and/or bottom current activity. Facies AD4 was interpreted as a facies representing the upward migration of fluids through the sediment column (Hogan et al., 2012).

Facies AV1–AV4 in the Vaigat were interpreted as partly erosive gravity-flow deposits derived from: (i) the deposition and remobilisation of glacimarine sediment settling from turbid meltwater plumes in the case of AV1 and AV4; (ii) an interplay of suspension settling and bottom currents in the case of AV2; and/or (iii) slumps down bedrock slopes in the case of AV3 (Hogan et al., 2012). Facies AV5 forms a conformable drape over the existing topography and was inferred to be deposited by post-glacial hemipelagic sedimentation with variable input of IRD by icebergs and sea ice (Hogan et al., 2012).

3. Materials and methods

Nine vibrocores (VC03–VC11) from Disko Bay and three from the Vaigat (VC12–VC14; Fig. 1c) were collected in August 2009 during cruise JR175 of the *RRS James Clark Ross* to the West Greenland continental margin. Together with swath-bathymetric data (Fig. 1b), these sediment cores provide the basis for this study. The cores were acquired using the British Geological Survey vibrocorer with a 6 m-long barrel and an inner diameter of approximately 9 cm. Core recovery was excellent in soft sediments to moderate in diamicts. Upon retrieval, all sediment cores were divided into $\sim$1 m long sections, split into working and archive halves, and stored at $+4°$C. Core locations and lengths are summarised in Table 1. In order to identify the lithofacies, core logs of all working halves were generated from the core sections, and x-radiographs were used to provide supplementary information on sub-surface sedimentary structures and quantification of clasts larger than 2 mm, classified as IRD (sensu Grobe, 1987). A GEOTEK multi-sensor core logger (MSCL) was used to measure physical properties such as wet-bulk density, p-wave velocity (only VC05, VC07, VC09) and magnetic susceptibility (MS), which was acquired with a Bartington point-sensor mounted on the GEOTEK system. Shear strength measurements were undertaken with a Durham Geo Slope Indicator torvane and, for most cores, were carried out directly after splitting in 2009. For VC03 and VC04, however, the shear strength was only determined in 2016; hence values for these cores should be treated as estimates. Grain-size distribution and water content were measured by sampling approximately 1 cm-thick sediment slices in 8 cm-intervals, which were weighed, dried at 60°C and subsequently weighed and sieved through mesh sizes of 63, 125, 250, and 500 μm.

Samples for radiocarbon dating were collected from as close to distinct lithological boundaries in the cores as possible. Accelerator Mass Spectrometry (AMS) radiocarbon dates were measured at Beta Analytic on ~6 mg of mixed species benthic foraminifera, and additional radiocarbon dates were obtained from molluscs and seaweed at the INSTAAR NSRL laboratory. The conventional radiocarbon ages were calibrated into cal a BP using Calib 7.1 with the MARINE13 curve and a reservoir correction of ΔR=140±25 (Stuiver & Reimer, 1993; Lloyd et al., 2011; Reimer et al., 2013). The same calibration was applied to already published ^{14}C dates from marine shells in Disko Bay (Lloyd et al., 2005; McCarthy, 2011; Ó Cofaigh et al., 2013), in order to make dates directly comparable.

Swath-bathymetric data were acquired during the same cruise, using a hull-mounted Kongsberg Maritime Simrad EM120 multibeam echo sounder. The system operates at a frequency of 12 kHz and was calibrated using sound velocity profiles for the water column obtained from XBTs. The data were processed using MB-System Software and QPS Fledermaus, gridded to a cell size of 30x30 m in QPS DMagic, and visualised and interpreted in Fledermaus. The data were supplemented with swath-bathymetric data collected during two additional cruises to Disko Bay, one on *RV Maria S. Merian* in June 2007, and

Table 1: Core locations and recovery.

Core ID	Latitude	Longitude	Area	Depth [m]	Length [m]
VC03	69°10.81' N	51°11.61' W	Disko	545	1.57
VC04	69°09.97' N	51°10.15' W	Disko	263	1.10
VC05	69°09.60' N	51°31.63' W	Disko	389	5.87
VC06	69°08.94' N	52°04.14' W	Disko	439	4.94
VC07	69°08.62' N	52°18.88' W	Disko	439	5.46
VC08	69°08.35' N	52°38.24' W	Disko	429	3.91
VC09	69°05.79' N	51°23.65' W	Disko	294	5.98
VC10	69°05.95' N	51°31.22' W	Disko	351	4.86
VC11	69°06.90' N	52°25.60' W	Disko	410	3.25
VC12	69°53.12' N	51°53.15' W	Vaigat	616	3.66
VC13	69°58.46' N	51°44.47' W	Vaigat	341	3.40
VC14	69°56.97' N	51°40.35' W	Vaigat	386	4.66

the other on the private fishing vessel *MV Smilla* in August 2008. The *Merian* data were acquired with a hull-mounted Kongsberg Maritime EM120 multibeam echo sounder in deep water and a Kongsberg Maritime EM1002 in shallow water, with the former operating at a frequency of 12 kHz and the latter at 95 kHz. The data were processed in the MB-System software (sensu Caress & Chayes, 1996) and gridded to a cell size of 24x24 m. The *MV Smilla* data were collected using a temporarily installed Sea Beam 1180 shallow water swath echo sounder system at a nominal frequency of 180 kHz, and gridded to a cell size of 15x15 m. Sub-bottom profiler data are also available for this study (Fig. 1c) and were gathered simultaneously with the swath bathymetry from the 2009 *James Clark Ross* cruise, using a Kongsberg Maritime TOPAS PS18 sub-bottom profiler, which operated at a frequency of 3.5 kHz. These data were played out in near-real time with an EPC chart recorder installed on board the vessel, providing high-resolution (30–40 cm) acoustic profiles, post-processed in the TOPAS Software, and subsequently loaded into IHS The Kingdom Software 2015. Conversion between milliseconds and metres was done using a p-wave velocity of 1610 m s^{-1}, the combined average velocity measured in unconsolidated sediments from the three cores from Disko Bay. The TOPAS data and parts of the swath-bathymetric data were already analysed and interpreted by Hogan et al. (2012) and TOPAS profiles are thus only used for correlation purposes in this study. Bathymetric data from the *Merian* and *Smilla* vessels were previously interpreted by Schumann et al. (2012).

4. Results

4.1. Swath bathymetry

A geomorphological map of the landforms in Disko Bay and the Vaigat Strait is shown in Figure 3. Earlier mapping from the easternmost part of Disko Bay (Hogan et al., 2012; Schumann et al., 2012) is incorporated into this map.

Large transverse ridges The most prominent characteristic of the seafloor is its rugged, irregular topography, imparted by a number of transverse ridges, which are generally orientated in a north-south direction (Fig. 3). Most of these ridges are relatively discontinuous and between 1 and 2 km long. They have sharp crests imparted by steep eastern, and more gradual western flanks, the majority of which are intensely streamlined in the direction of ice flow (generally east-west). Three ridges, R1–R3, stand out morphologically (Fig. 3). R1 is the most proximal ridge, concave in planform with respect to the ice margin, and located approximately 20 km west of Isfjeldsbanken. It is $\sim$4.5 km long, 40 m high, and up to 500 m wide. R2, at 26 km from Isfjeldsbanken, is 20 km long, 200–1000 m wide, and 10–120 m high, with a generally convex crest forming a slight zig-zag pattern (Fig. 4). The distal flanks of R1 and parts of R2 are intensely streamlined (Fig. 4). R3 is curvilinear in plan view, 20 km long, up to 4 km wide and 20–120 m high.

The large dimensions and the rugged appearance of R1–R3 indicate that a purely glacial origin is unlikely (cf. Ottesen & Dowdeswell, 2006; Ottesen et al., 2008; Hogan et al., 2011; Flink et al., 2015; Streuff et al., 2015), and the sub-bottom profiler data show that the majority of the topographically distinct highs are formed in bedrock (e.g. Fig. 4d). We therefore interpret these ridges as bedrock highs that were overridden and streamlined by glacial ice.

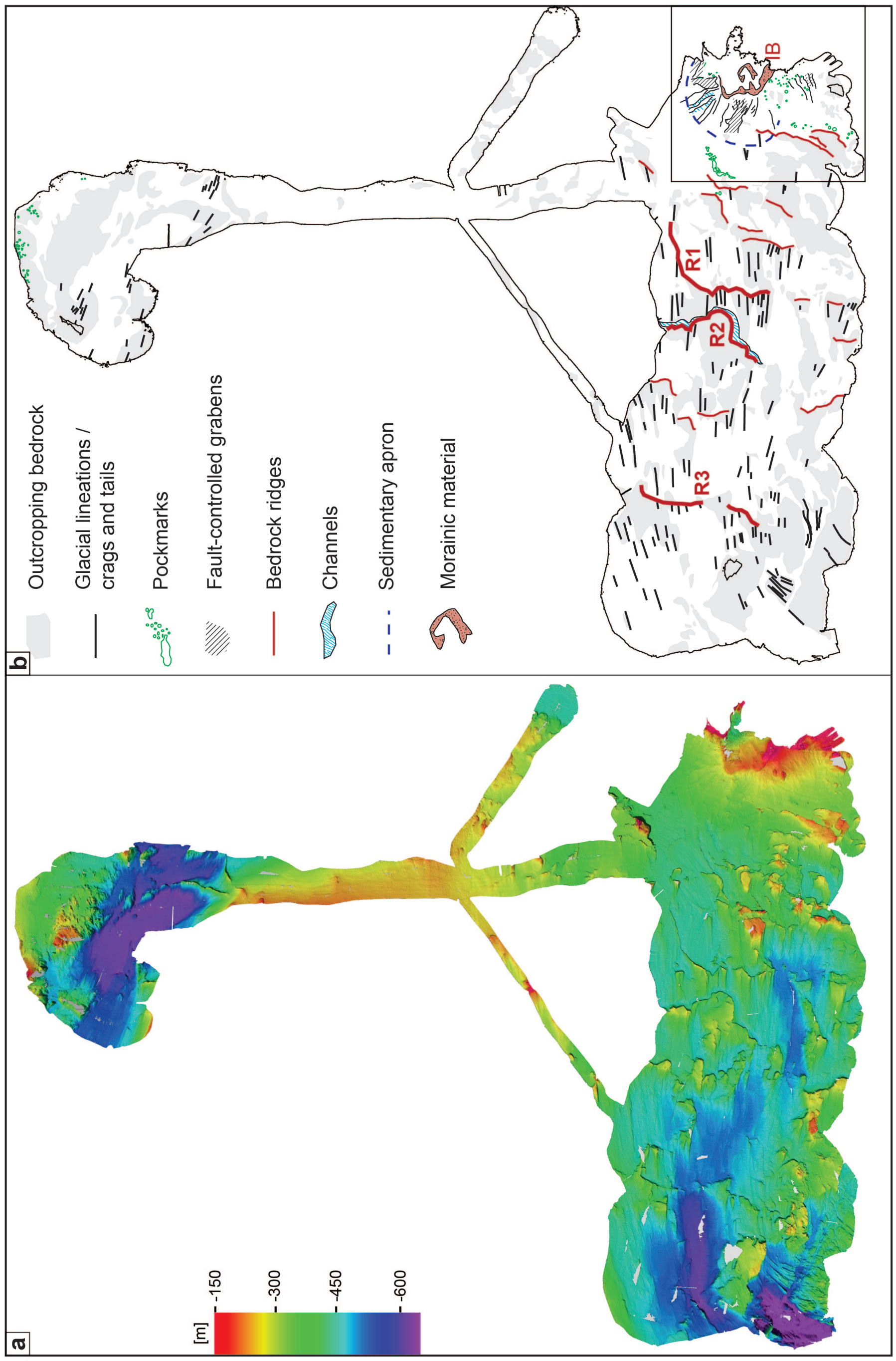

Figure 3: a) Bathymetry in Disko Bay and the Vaigat Strait. b) Geomorphological map of all the landforms in Disko Bay. Landforms in the black rectangle indicate those already mapped by Hogan et al. (2012) and Schumann et al. (2012). IB = Isfjeldsbanken. Detailed examples are shown in Fig. 4.

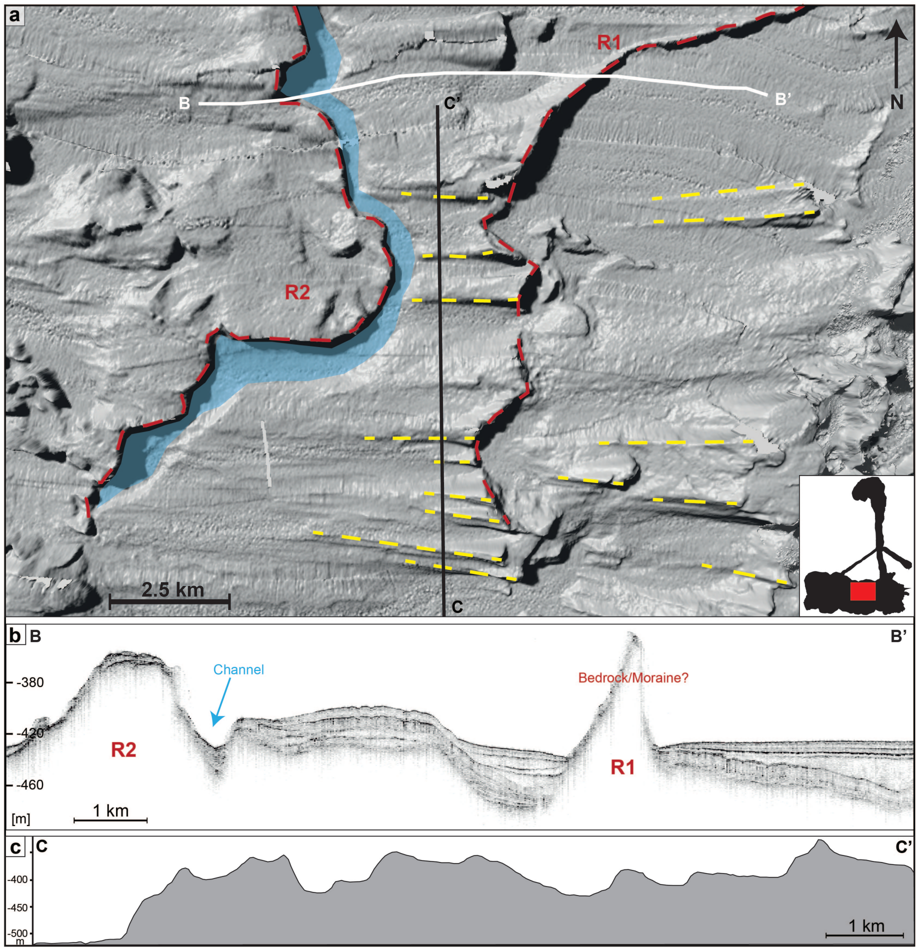

Figure 4: a) Shaded-relief image of the bathymetry in Disko Bay. Red lines show the location of bedrock ridges, while yellow stippled lines follow the long-axes of the crags and tails. The blue polygon shows the location and extent of C1, and the red rectangle on top of the black polygon in the bottom-right hand corner shows the extent and location of a). b) TOPAS profile BT–BT' across across a submarine channel and a ridge. c) Bathymetric profile C–C' across crag-and-tails.

Elongate hills The north-south orientated bedrock ridges in Disko Bay are closely associated with east-west orientated elongate hills (Figs. 3, 4). The latter are 1.5–7 km long, 100–1000 m wide, and around 10 m high with typically broader, steeper stoss sides and gently tapering lee ends (Fig. 4). The characteristics of these landforms are consistent with formation as crag-and-tails, the presence of which in Disko Bay was also documented by Ó Cofaigh et al. (2013). Crag-and-tails form subglacially and in association with bedrock highs, where the crag consists of bedrock with a lee-side tail forming from deposition of unconsolidated subglacial sediment (Dionne, 1987; Stokes et al., 2011).

Submarine channels A large channel, C1, occurs about 25 km west of Isfjeldsbanken and is ~16 km long, around 800 m wide and up to 40 m deep. It follows the eastern edge of R2 and is sinuous in planform (Fig. 4). Several similar, generally smaller depressions have also been observed along the western flank of Isfjeldsbanken (Fig. 3; Hogan et al., 2012). The large channel C1 is interpreted to be a subglacial channel eroded by meltwater flowing beneath an extended Jakobshavn Isbræ (cf. e.g. Walder & Hallet, 1979). The depth and shape of the channel imply that its formation took some time, during which meltwater erosion must have been focussed along R2. Assuming that meltwater disperses with increasing distance from the ice margin, concentrated meltwater routing implies that the ice margin was relatively close. As the channel is located on the proximal side and follows the line of R2, it seems plausible that the glacier front grounded on the bedrock high for an extended period of time and subglacial meltwater was routed around the bedrock obstacle eroding the channel. The smaller channels on the western flank of Isfjeldsbanken formed in the sediment pile and are interpreted as submarine channels eroded from downslope sediment-gravity flows, occasionally promoted by the presence of faults (Hogan et al., 2012).

Sediment-gravity flows A large sedimentary apron on the western flank of Isfjeldsbanken was described by Schumann et al. (2012) and several smaller incisions along the same flank were interpreted as sediment slumps from downslope-gravity flows (Hogan et al., 2012). Although such landforms do not always appear clearly on our bathymetric data, the sub-bottom profiler data indicate the abundance of such deposits in Disko Bay and the Vaigat Strait (see AD2 and

AV1–AV5 in Fig. 2). Common triggers of gravity-flows are, for example, continuously high sediment accumulation and regional seismicity, the latter possibly related to isostatic rebound (e.g. Hunt & Malin, 1998; Forwick & Vorren, 2012).

Pockmarks Several circular depressions occur in Disko Bay, and are especially common in the eastern part of the bay and on the distal flank of Isfjeldsbanken (Fig. 3; see also Figs. 6 and 8 in Hogan et al., 2012). The depressions often occur in clusters, are between 5 and 300 m in diameter, and 7–30 m deep. On the sub-bottom profiler data, the depressions are associated with a drawdown of the overlying reflections and occasional acoustic masking (Hogan et al., 2012). These depressions are interpreted as pockmarks (Hogan et al., 2012), which are formed as a result of gas or pore fluid seepage (e.g. Harrington, 1985; Hovland & Judd, 1988; Forwick et al., 2009; Nielsen et al., 2014; Dowdeswell et al., 2016). Acoustic masking on the sub-bottom profiler data supports this interpretation.

4.2. Sub-bottom profiler data

Description Our seismostratigraphic findings support previous work from Hogan et al. (2012), who identified four acoustic facies in Disko Bay, AD1–AD4. Although difficult to discern, we identify one additional acoustic facies, AD5, which conformably overlies and occasionally onlaps the acoustic basement in localised areas of Disko Bay (see Figs. 2a, b, 5c, f). AD5 is characterised by chaotic, semi-transparent internal reflections of variable strength and is 11 ms ($\sim$9 m) at its thickest. It can be bounded by a strong upper reflector and can appear slightly distorted by bedrock echos (Fig. 2a). AD5 differs from AD2 by a slightly more opaque acoustic character with a larger number of internal reflections. Furthermore, unlike in AD2, the TOPAS signal weakens with increasing depth and quickly disappears beneath the upper boundary of AD5.

Interpretation The semi-transparent and internally massive acoustic appearance of Facies AD5 as well as a decreasing signal strength with depth have sometimes been attributed to uniformly mixed sediments of possibly diamictic composition (Stewart & Stoker, 1990; Forwick & Vorren, 2011). AD5 could thus represent a diamict deposited either at or beneath the glacier grounding line as glacial till, or from increased iceberg-rainout. Our sedimentary data indicate that the diamict is more likely related to deposition from glacimarine processes (see LD1, section 4.3 below), but based on the partly distorted signal on the sub-bottom profiler data and a limited penetration depth of the cores into AD5, a clear distinction cannot be made.

4.3. Lithological data

4.3.1. Lithofacies

From the sedimentary record preserved in the vibrocores we define five lithofacies in Disko Bay (LD1–LD5), and one in the Vaigat (LV1). The correlation between lithology and sub-bottom profiler data is shown in Figure 5. Physical properties of the lithofacies and their stratigraphic distribution within the cores are displayed in Figures 6 and 8, while examples of the x-radiographs for each facies are shown in Figure 7.

LD1 is a dense (2–3 g cm^{-3}), matrix-supported diamict with a predominantly sandy matrix, and a majority of sub-angular to sub-rounded clasts (Fig. 7). Based on differences in shear strength and sediment structure, we distinguish LD1a and LD1b. LD1a shows some contortions on x-radiographs (Fig. 7), has a shear strength of up to 40 kPa, and only occurs in VC08 (Fig. 6). LD1b is massive, has a shear strength of up to 70 kPa, and only occurs in VC03 and VC04. The water content and the proportion of clay and silt in both lithofacies of LD1 are low with values around 20% and 40%, respectively (Fig. 6). Around 30-40% of the grains are >250 μm, with generally 5–10 clasts > 2 mm occurring per 2 cm-window. The MS is around 100 x 10^{-5} SI on average and shows distinct peaks. LD1b is part of AD5 (Fig. 5), but strong bedrock reflection hyperbolae on the TOPAS signal around the core site of VC08 prevented a direct correlation between LD1a and its acoustic counterpart.

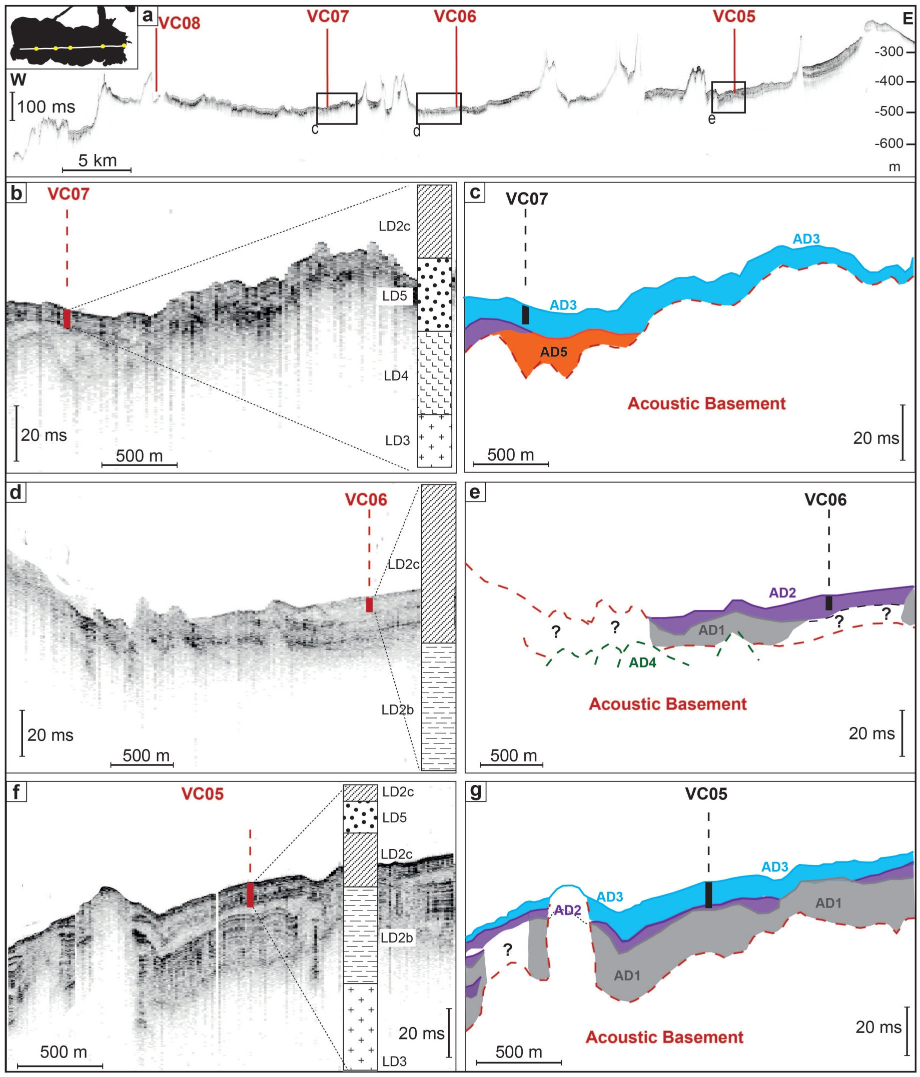

Figure 5: a) TOPAS profile across the core locations. The black polygon indicates location and extent of the profile. b), d), f) TOPAS lines across VC07, VC06, and VC05, respectively, with c), e), g) showing the according acoustic facies interpretation with respect to core penetration.

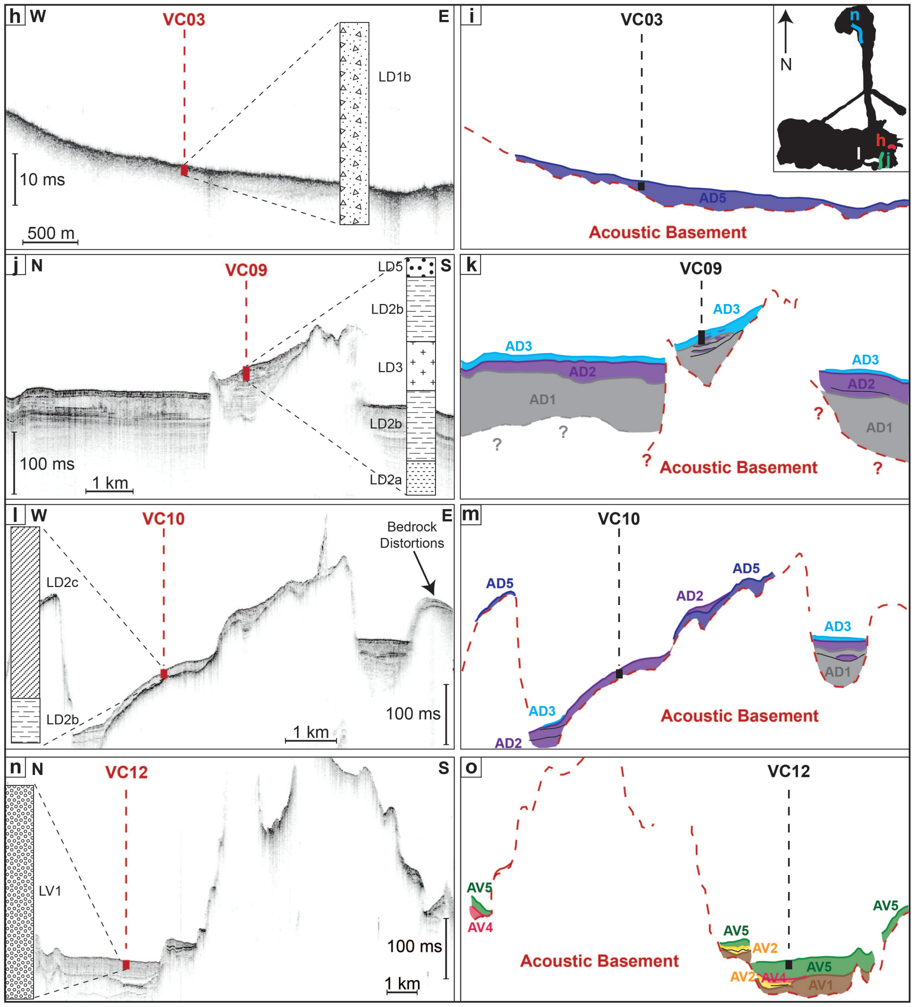

Figure 5 (cont.): TOPAS lines across and acoustic facies interpretation at the core sites of h), i) VC03, j), k) VC09, l), m) VC10, and n), o) VC12 from the Vaigat Strait. Black polygon in the top right-hand corner of i) shows the location of the TOPAS lines with respect to the bathymetry.

Lithofacies LD2 contains mud with highly variable amounts of clasts and is present in all cores from Disko Bay (Fig. 6). Clasts are pebble- to gravel-sized, mainly sub-angular to sub-rounded and of predominantly granitic composition, presumably sourced from the Precambrian basement (Fig. 7; cf. Chalmers et al., 1999; Larsen & Pulvertaft, 2000; Weidick & Bennike, 2007). The matrix is composed of clay and silt and varies in colour between (dark) greenish grey (Munsell colour code: GLEY 1 4/10Y to 5/10Y) and greenish grey (GLEY 1 5/10Y to 6/10Y) or dark to olive grey (5Y 4/1 to 4/2). The muds have a density of 1–2 g cm^{-3} and a shear strength between 2 and 10 kPa, which slightly increases down-core (Fig. 6). LD2 has a water content between 30 and 60% (Fig. 6) and standing water was observed on localised areas of the sediment surface. The mud fraction generally exceeds 90% but can drop to 80% where clasts are abundant (Fig. 6). Clast concentrations are up to 25 clasts per 2 cm-window. The facies has a highly variable MS between ~15 and 150 x 10^{-5} SI (Fig. 6). We distinguish subfacies LD2a, LD2b, and LD2c. In LD2a, which only occurs at the bottom of VC09, the mud appears diffusely stratified with some pebble-sized clasts and occasional bioturbation burrows at the top of the facies (Figs. 6, 7). LD2b contains internally massive mud in stratified sequences, with strata between ~4 and 15 cm thick. The strata have generally sharp contacts in the lower parts of LD2b, and more diffuse boundaries, partly promoted by bioturbation, in the upper parts (Figs. 6, 7). LD2c contains massive, occasionally bioturbated mud (Fig. 7). LD2 correlates with acoustic facies AD2 and AD3 (Fig. 5).

Lithofacies LD3 is composed of massive and partly contorted mud, interspersed with massive fine sand-rich units (Fig. 6). These units are occasional to frequent, mostly inclined, and occur as mm-thick laminae or cm-thick layers with sometimes sharp, but mostly diffuse lower boundaries (Fig. 7). In places the sandy beds are heavily contorted (Fig. 7). The overall density of LD3 is around 1.6 g cm^{-3} with minor variations, whereas the shear strength is highly variable (0.5 and 12 kPa; Fig. 6). Water content is around 20–30%, and grain size distribution varies according to the sub-sampled lithology, with >95% clay and silt in the matrix, and ~80% clay and silt in the sandy layers (Fig. 6). IRD grains >2 mm are rare. The MS is ~100–120 x 10^{-5} SI with few localised and distinct peaks. The facies occurs in either the basal or middle parts of VC05, VC07, and VC09 (Fig. 6). LD3 forms part of the acoustic facies AD2 (Fig. 5).

Lithofacies LD4 contains diffusely laminated mud interbedded with diamictic

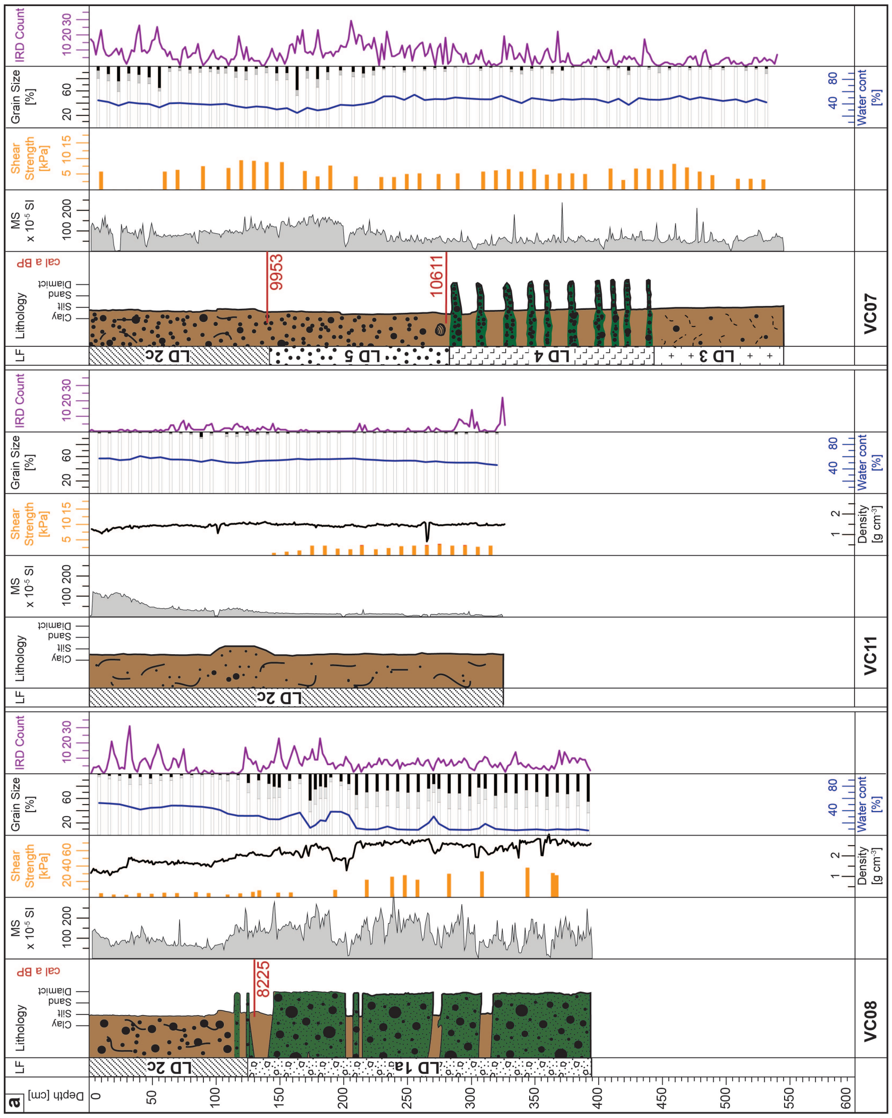

Figure 6: a) Lithological and lithofacies logs with physical properties of vibrocores VC08, VC11, and VC07 from Disko Bay (west to east). MS = magnetic susceptibility. Note the different scales for the shear strength. Grain-size distribution results were grouped thus: white bars = grains <63 μm, grey bars = 63–250 μm, black bars = grains > 250 μm.

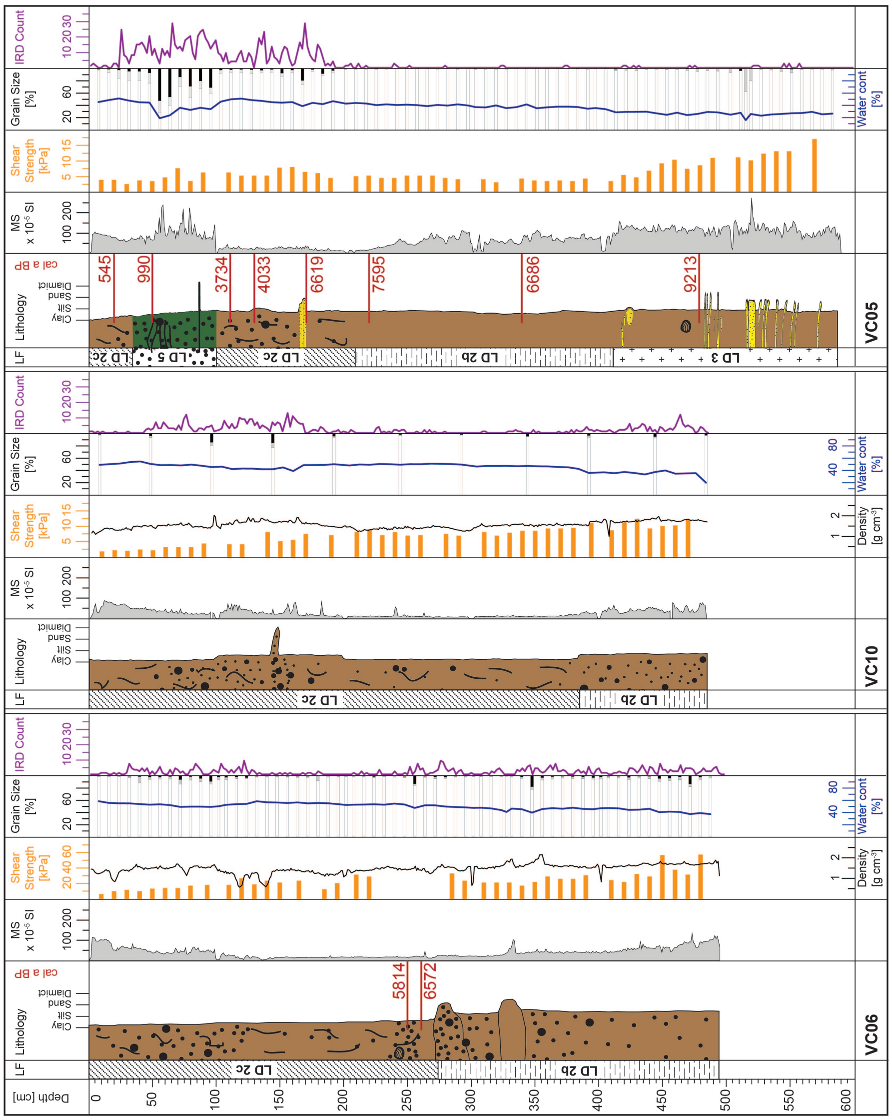

Figure 6 (cont.): Lithological and lithofacies logs with physical properties of vibrocores VC06, VC10, and VC05 from Disko Bay (west to east). MS = magnetic susceptibility. Grain-size distribution: white bars = grains <63 μm, grey bars = 63–250 μm, black bars = grains > 250 μm.

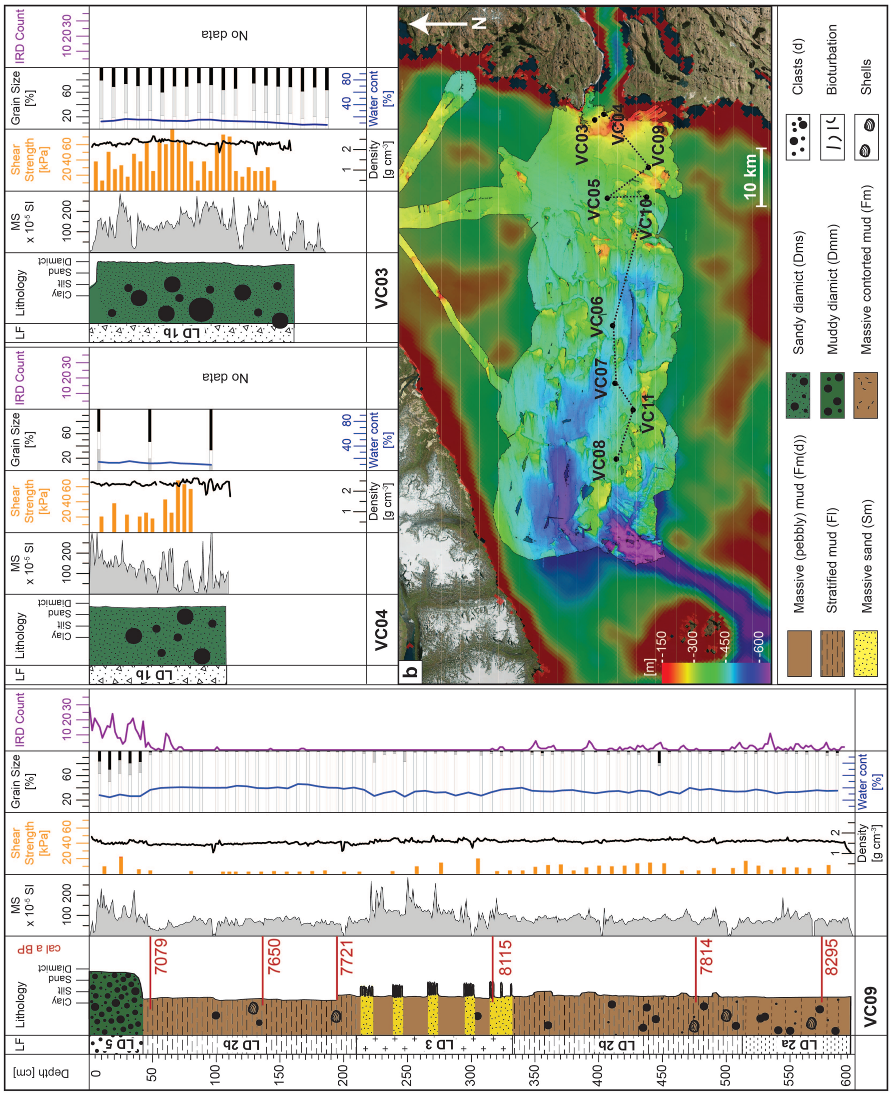

Figure 6 (cont.): Lithological and lithofacies logs with physical properties of vibrocores VC09, VC04, and VC03 from Disko Bay (west to east). MS = magnetic susceptibility. b) Core locations. The black stippled line indicates the order in which cores are shown. Grain-size distribution: white bars = grains <63 μm, grey bars = 63–250 μm, black bars = grains > 250 μm.

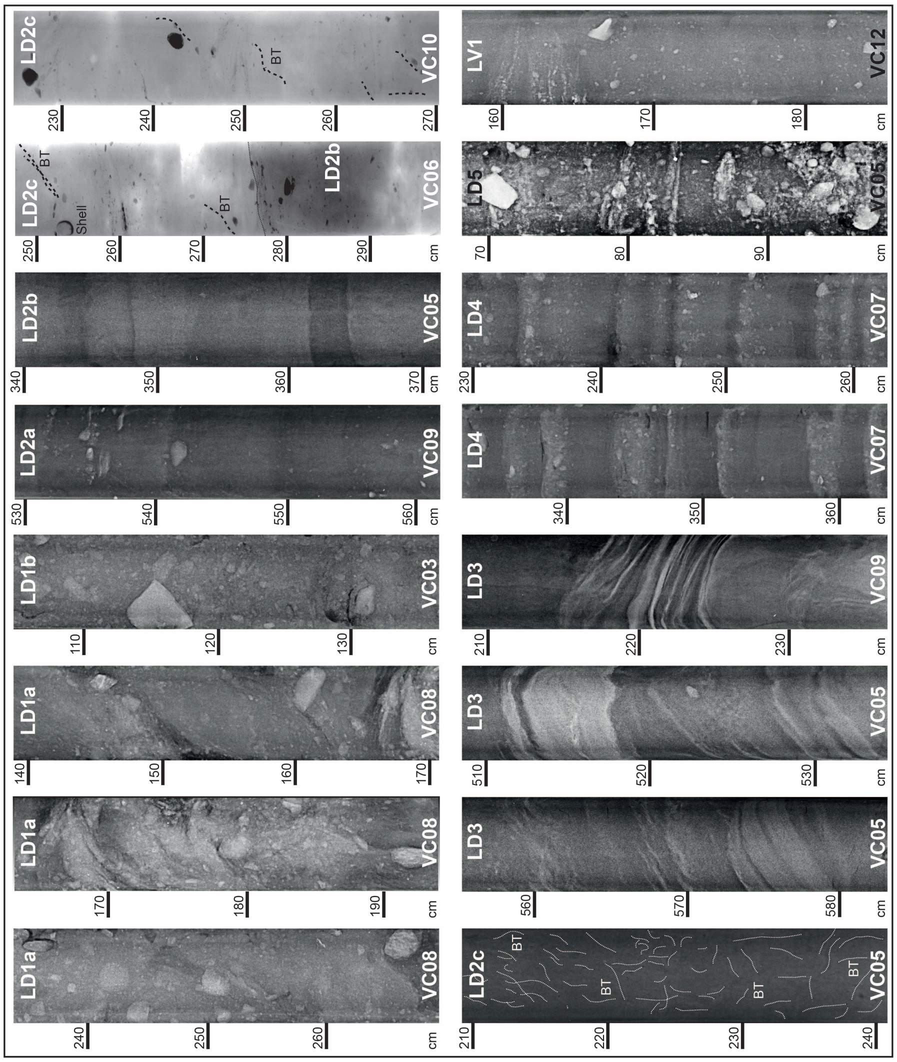

Figure 7: Examples of the x-radiographs from the six lithofacies LD1–LD5, and LV1 from different vibrocores (VC) and sediment depths in Disko Bay and the Vaigat Strait. Generally denser parts appear lighter, except for in the two x-radiographs from VC10 and VC06, where colours are reversed.

layers (Figs. 6, 7). The diamict layers are up to 4 cm thick, contain fines, sand, and pebbles, and normally have a very gradual and diffuse lower boundary, but a sharper upper contact, which is especially pronounced in the bottom parts of LD4 (Fig. 7). The shear strength is around 8 kPa, the water content $\sim$40%, and >90% of the sediment are <63μm. The increased clast content in the diamictic layers is reflected in a variable IRD count of up to 21 clasts per 2 cm (Fig. 6). Minor oscillations in MS, which is generally $\sim$50 x 10^{-5}, are interrupted by several pronounced peaks to values between 125 and 225 x 10^{-5} SI (Fig. 6). LD4 is present only in VC07 (Fig. 6).

Lithofacies LD5 is a matrix-supported diamict, with a mud-dominated matrix (rather than sand-dominated as for LD1) and abundant angular to subangular clasts of variable diameter (Fig. 7). Smaller pebbles are sometimes concentrated in dense, cm-thick beds, which have sharp contacts with the surrounding sediments. The density is around 1.5 g cm^{-3}, the shear strength between 5 and 10 kPa, and the water content between 10 and 40%. LD5 has a variable proportion (20–80%) of fines (<63 μm) and a high IRD count of up to 25 clasts per 2 cm-window. A spiky appearance with numerous well-pronounced peaks defines the MS, which, in most cases, exceeds 80 x 10^{-5} SI.

The cores from the Vaigat contain a single lithofacies, LV1, which comprises massive, dark grey to dark olive grey mud (5Y 4/1 to 3/2) with a moderate clast abundance (Figs. 7, 8). It is similar to LD2a from the cores in Disko Bay, but the matrix contains low amounts of sand and there is no evidence of bioturbation. Internal sedimentary structures are absent, with the exception of occasional laminae of coarser grains (medium sand to pebble-sized; Fig. 7). The density is around 1.5 g cm^{-3} and the shear strength 4–12 kPa, with a slight increasing trend down-facies (Fig. 8). LV1 has a water content of $\sim$50% and >95% fines and occurs in all three cores from the Vaigat (Fig. 8). The IRD count is highly variable with 0–22 clasts per 2 cm-window, and the MS is generally around 200–250 x 10^{-5} SI with relatively minor variations (Fig. 8). LV1 forms part of acoustic facies AV5 (Fig. 5).

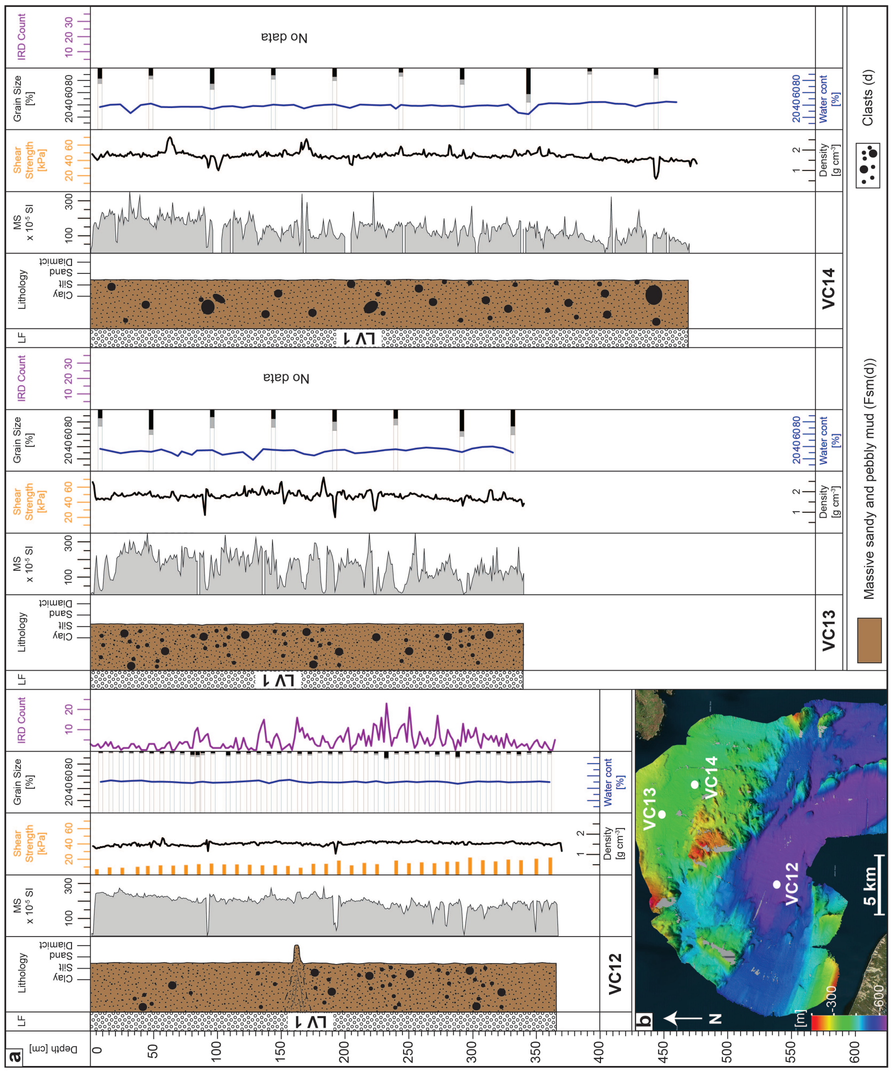

Figure 8: Lithological and lithofacies logs of the three vibrocores from the Vaigat Strait and their physical properties. MS = magnetic susceptibility. Grain-size distribution: white bars = grains <63 μm, grey bars = 63–250 μm, black bars = grains > 250 μm.

4.3.2. Radiocarbon dates and sediment accumulation rates

Table 2: Radiocarbon dates and calibrated ages used in this study. Unless otherwise specified all bivalves were intact and did not show evidence of being re-worked.

Core ID	Depth [cm]	Lab Code	Sample	Reported age [^{14}C a BP]	Mean probability age [cal a BP]	2σ [cal a BP]
VC05	20–21	AA–90391	Seaweed	1079 ± 78	545	418–668
VC05	50–51	AA–90392	Seaweed	1575 ± 88	990	778–1190
VC05	112–113	Beta–434927	Seaweed	3930 ± 30	3734	3612–3845
VC05	130–131	AA–90393	Seaweed	4159 ± 50	4033	3872–4210
VC05	170–171	AA–90394	Seaweed	6322 ± 60	6619	6451–6776
VC05	220–221	AA–90395	Seaweed	7250 ± 380	7595	6788–8355
VC05	340–341	AA–90396	Seaweed	6370 ± 180	6686	6294–7119
VC05	478–479	AA–90396	Paired Bivalve	8710 ± 50	9213	9045–9383
VC06	250	Beta–434928	Single Bivalve	5580 ± 30	5814	5711–5905
VC06	272–273	Beta–434929	Seaweed	6280 ± 30	6572	6456–6672
VC07	140–142	Beta–434930	Foraminifera	9300 ± 30	9953	9772–10118
VC07	280–281	Beta–434931	Paired Bivalve	9850 ± 30	10611	10503–10723
VC08	130–132	Beta–434932	Foraminifera	7890 ± 30	8225	8130–8326
VC09	48	Beta–434933	Seaweed	6700 ± 30	7079	6955–7184
VC09	137	Beta–434934	Paired Bivalve	7330 ± 30	7650	7570–7743
VC09	195	Beta–434935	Paired Bivalve	7400 ± 30	7721	7631–7821
VC09	316–318	Beta–434936	Foraminifera	7800 ± 30	8115	8001–8214
VC09	476	Beta–265208	Paired Bivalve	7490 ± 50	7814	7684–7928
VC09	575	Beta–265209	Paired Bivalve	7970 ± 50	8295	8171–8394

Radiocarbon dates presented here are rounded to the closest 100 years and are shown in detail in Table 2 and Figure 9. AMS measurements were carried out on paired or whole bivalve shells (Table 2) or mixed benthic foraminifera taken from seemingly undisturbed sediment sections to ensure accuracy of the radiocarbon dates. The exception is the date at 316 cm in VC09, where the frequent sandy deposits most likely represent turbidites and the obtained date may hence derive from reworked material (see section 4.3.3 below). Other AMS measurements were carried out on seaweed taken from near the centre of the split cores to reduce the risk of material having been dragged down-core during the coring process. Notwithstanding this, the age reversal and the large error margin for the sample from 340 cm in VC05 indicate that the seaweed at this depth was not in-situ. Sediment accumulation rates (SARs; Fig. 9) were calculated from the mean radiocarbon ages and assume constant accumulation between each date.

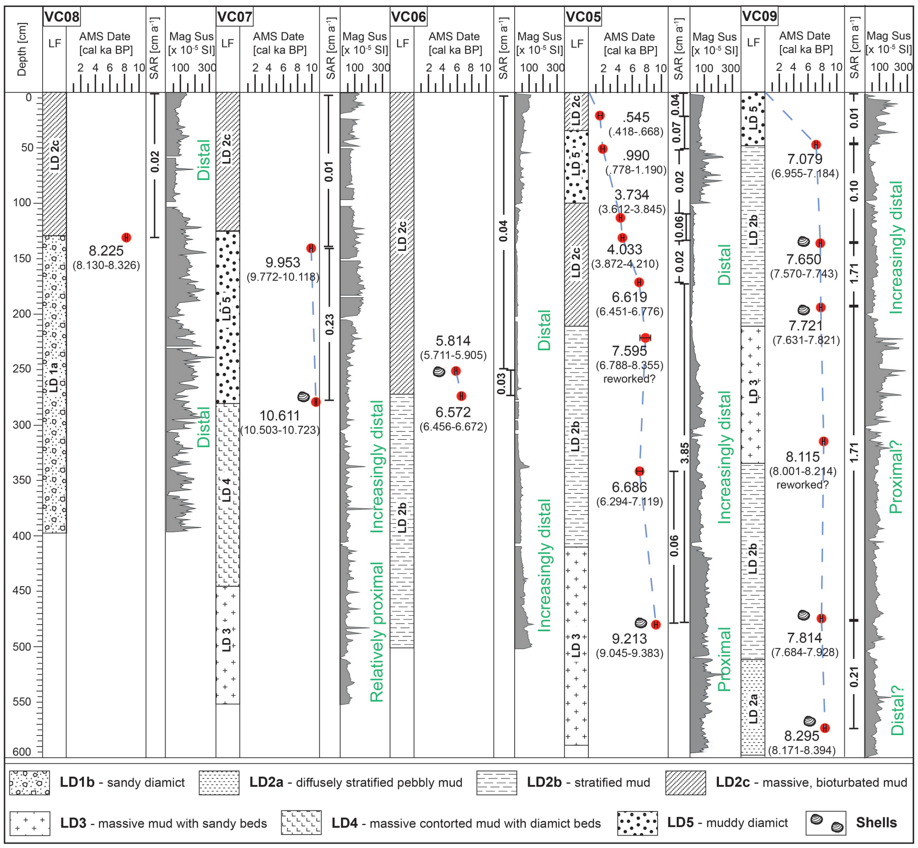

Figure 9: Lithofacies logs with radiocarbon dates (error bars indicate 2σ-range) and calculated SARs from a core transect across Disko Bay from west to east (see Fig. 6b for core locations). Note that core signatures are only used as a means to visually differentiate between lithofacies, not to describe the actual lithology. For details on the lithological composition of the cores and lithofacies see also Fig. 6 and section 4.3. Together with the MS these values give an idea about the glacimarine environment the lithofacies were deposited in.

Radiocarbon dating suggests that LD1a at the base of VC08 was deposited prior to ~8.2 cal ka BP and that the overlying LD2c accumulated at an average rate of 0.02 cm a^{-1} (Fig. 9). Basal sediments in VC07 contain LD3 and LD4 and are the oldest recovered from Disko Bay, deposited before 10.6 cal ka BP. The top of the overlying LD5 dates to ∼9.9 cal ka BP, implying a SAR of 0.23 cm a^{-1} for this facies (Fig. 9). The same date suggests that the topmost facies in VC07, LD2c, was deposited afterwards at a SAR of 0.01 cm a^{-1}. Two dates from VC06 indicate that its bottom part (LD2b) is older than ∼6.5 cal ka BP, and that the overlying LD2c accumulated at a rate of 0.03–0.04 cm a^{-1} (Fig. 9). LD3 at the bottom of VC05 was deposited around 9.2 cal ka BP. Assuming that the date of 7.6 cal ka BP at the top of the overlying LD2b is indeed unreliable, LD2b accumulated from before 6.7 to just before 6.6 cal ka BP at a rate of ∼0.05 cm a^{-1} (Fig. 9). The overlying LD2c was deposited until today, at a rate of 0.02–0.06 cm a^{-1}, but deposition was interrupted from ∼3.7 until after 0.99 cal ka BP, during which time LD5 formed (Fig. 9). The bottom half of VC09 (LD2a, LD2b and LD3) was deposited between 8.3 and 7.7 cal ka BP at an SAR of 0.21–1.71 cm a^{-1} (Fig. 9). In the top half of the core LD2b accumulated between 7.7 and 7.0 cal ka BP at decreasing rates between 1.72 and 0.10 cm a^{-1}, and is overlain by LD5, deposited since 7.0 cal ka BP at a very low SAR of 0.01 cm a^{-1} (Fig. 9).

4.3.3. Interpretation

LD1 – sandy diamict

Although x-radiographs of LD1 are similar to glacial till documented from outer Disko Bay and the continental shelf in the Disko and Uummannaq Troughs (Ó Cofaigh et al., 2013; Dowdeswell et al., 2014; Hogan et al., 2016; Sheldon et al., 2016) and the shear strength of ∼40–80 kPa exceeds that of subglacial tills from Antarctica (cf. Ó Cofaigh et al., 2005), the absence of planar structures or indications of clast alignment in both, LD1a and LD1b appear to be at odds with an interpretation as glacial till. Furthermore, in the case of LD1a, we would expect glacial till to be significantly older than the given age of 8.2 cal ka BP, considering that the bay was probably ice-free around 10 cal ka BP (Lloyd et al., 2005; Young et al., 2011a). In the case of LD1b, we would expect any sequence of glacial till to be covered by a succession of Holocene sediments, as till could only have formed at the core sites when the ice margin last paused at Isfjeldsbanken, around 10 ka BP. We therefore favour an interpretation of LD1a as a mass-flow deposit and of LD1b as post-glacial glacimarine sediments, where deposition occurred from meltwater and/or the water column and melting icebergs (e.g. Elverhøi et al., 1980, 1983; Gilbert, 1983; Hogan et al., 2016). The partly contorted appearance of LD1a in VC08 and the occurrence of mud strata within the facies indicate sediment reworking and suggest that LD1a was formed as a gravity-flow deposit reworking glacimarine mud and IRD (cf. e.g. Kuenen, 1948; Shanmugam et al., 1994; Forsberg et al., 1999). This seems reasonable, as the core site of VC08 is located in a submarine basin between two bedrock highs, the steep slopes of which could have promoted repeated mass-flows. Indeed, the sub-bottom profiler data show abundant mass-flow deposits in Disko Bay, supporting an interpretation of LD1a as a gravity-flow deposit. This interpretation is also consistent with the low shear strength and the comparatively young age of LD1a. An interpretation of LD1b as post-glacial IRD-rich sediment is based on the fact that VC03 and VC04, containing LD1b, were taken from the top of Isfjeldsbanken, where the high accumulation of IRD is likely, because (1) all icebergs calved off Jakobshavn Isbræ pass through Isfjorden into Disko Bay, and (2) the sill traps larger icebergs inside the fjord due to the shallow water depth (Echelmeyer et al., 1991; Hogan et al., 2011). These bergs need to melt considerably before passing into Disko Bay (Echelmeyer et al., 1991; Hogan et al., 2011), and thus probably deposit the majority of their debris at or near Isfjeldsbanken. Although no distinct iceberg ploughmarks were observed on the swath-bathymetric data, the relatively high shear strength in LD1b indicates that icebergs may have grounded at the core sites, scouring, compacting and homogenising the deposited sediments. Indeed, LD1b is macroscopically similar to diamicts in East Greenland, which have been interpreted as "iceberg turbates" (Vorren et al., 1983; Marienfeld, 1992; Dowdeswell et al., 1994; Linch & Dowdeswell, 2016).

LD2 – massive to stratified mud

LD2 is interpreted as glacimarine mud settling from suspension in glacial meltwater plumes and the water column (cf. e.g. Gilbert, 1983; Elverhøi et al., 1983; Dowdeswell et al., 1998; Ashley & Smith, 2000). Clasts record the deposition of IRD from icebergs and/or sea ice. The low shear strength and high water content of this facies support this interpretation.

Stratification in LD2a and LD2b is likely related to changes in depositional environment or sediment source. These are controlled by a number of factors, including e.g. regional warming and melting of the ice sheet, variability in the position of meltwater efflux, inter-annual variations in meltwater flux due to seasonal or tidal controls or floods from glacial lakes, or by ice-margin fluctuations controlling the proximity of the core site to the ice margin. The diffuse nature of the stratification in LD2a is thought to reflect a relatively ice-distal environment, where such changes have a smaller impact on the sedimentary record. An upward increase in bioturbation and the low SAR of 0.2 cm a^{-1} support an interpretation of LD2a as glacimarine mud deposited under (increasingly) distal conditions. Conversely, the distinct stratification in LD2b is thought to be indicative of a more glacier-proximal depositional environment. Ice-proximal conditions are supported by a high concentration of meltwater-derived fines, also reflected in SARs of up to 1.7 cm a^{-1}, an increased MS suggesting a predominantly terrestrial input (Steenfelt et al., 1990; Robinson, 1993; Møller et al., 2006; Seidenkrantz et al., 2013), and the lack of IRD, as under these conditions the input from icebergs is often masked by the fast accumulation of meltwater-derived fines (e.g. Elverhøi et al., 1980; Dowdeswell & Dowdeswell, 1989; Cowan et al., 1997; Gilbert et al., 2002). Radiocarbon dates show that LD2a was deposited some time after 8.2 cal ka BP, and accordingly the change from more distal to more proximal conditions between LD2a and LD2b in VC09 possibly reflects a re-advance of Jakobshavn Isbræ in response to the 8.2 ka cooling event (Weidick & Bennike, 2007; Young et al., 2011a, 2013). LD2b was deposited prior to 7.6 cal ka BP in VC05 and between ∼7.8 and 7.1 cal ka BP in VC09 (interrupted by deposition of LD3 just before 7.7 cal ka BP, Fig. 9). During this time

Jakobshavn Isbræ was at Isfjeldsbanken and began retreating into Isfjorden, which could have resulted in minor oscillations in the position of the ice margin causing the stratification in LD2b. However, deposition of LD2b also coincides with a period of strongly increased meltwater discharge, presumably caused by extensive thinning of the ice sheet prior to 8.3 ka BP (Rinterknecht et al., 2009; Seidenkrantz et al., 2013). Stratification would then have been imparted by inter-seasonal variations in meltwater flux to the core site, as the large variability in strata thickness within LD2b is at odds with the rhythmic stratification usually observed in seasonally-controlled meltwater deposits (cf. e.g. Domack, 1984; Mackiewicz et al., 1984; Ó Cofaigh & Dowdeswell, 2001). Although both scenarios are possible for the deposition of LD2b, we favour the former possibility and suggest that LD2b was deposited in a glacier-proximal environment where stratification was caused by minor ice front oscillations. This is based on several reasons, including that: (1) the occurrence of presumably distal glacimarine mud (LD2a) at the bottom of VC09 around 8.2 cal ka BP is strange given that enhanced meltwater release started as early as 8.6 ka BP in some regions, (2) lithological evidence from Disko Bay showed that the meltwater event had ceased by 7.7–7.5 ka BP (Seidenkrantz et al., 2013), yet deposition of LD2b and hence a strong meltwater signal prevailed until 7.0 cal ka BP in VC09, and even until 6.6 cal ka BP in VC06, and (3) if the meltwater event was responsible for the deposition of LD2b, the deposition of LD3 in between two packages of LD2b in VC09 (Fig. 9) would be difficult to understand (see also below). Furthermore, the traces of bioturbation at the top of LD2b and the declining MS and SARs up-facies are more easily accounted for by gradual ice margin retreat rather than a drastic reduction in meltwater flux. Ongoing retreat could also have led to an increasing amount of sediment being trapped behind the sill in Isfjorden, thus causing additional variability in the depositional environment at the core sites.

Based on its massive structure and the presence of bioturbation burrows suggesting favourable living conditions for some benthic organisms, LD2c is interpreted as ice-distal glacimarine mud. This is in accordance with the radiocarbon dates, which provide evidence for deposition of LD2c after ∼6.7 cal ka BP in VC05, during which time ice was retreating through Isfjorden (e.g. Lloyd et al., 2005; Weidick & Bennike, 2007; Hogan et al., 2011). The switch from ice-proximal (LD2b) to ice-distal conditions (LD2c) between ∼6.7 and 7.6 cal ka BP in VC05 and around 7.1 cal ka BP in VC05 and VC09, respectively, show that by this time Jakobshavn Isbræ had retreated so far into Isfjorden, that meltwater sedimentation was no longer the dominant process at the core sites. The stratigraphic position of LD2c at the top of most cores from Disko Bay, the low SAR of ∼0.2 cm a^{-1}, and the low MS indicating a predominantly hemipelagic origin (cf. Steenfelt et al., 1990; Møller et al., 2006; Seidenkrantz et al., 2013) support this interpretation (e.g. Syvitski & Murray, 1981; Gilbert, 1982; Boulton, 1990; Sexton et al., 1992). Indeed, the ice margin is thought to have retreated behind its present position during the mid-Holocene, where it remained until ∼2.2 ka BP (Weidick & Bennike, 2007). However, the gradual increase in MS in the top 50 cm of LD2c in most cores from Disko Bay, and the simultaneous increase in SARs in VC05 and VC06 (Fig. 9) suggest a terrestrial origin for the youngest sediments in Disko Bay and a relatively higher availability of meltwater-derived fines. This could be related to the westward re-advance of the ice margin after 2.2 ka BP and/or the recent increase of thinning and subglacial melting of Jakobshavn Isbræ and adjacent GIS outlets (Holland et al., 2008; Rignot et al., 2010).

LD3 – stratified mud with sand laminae

The stratified fine-grained mud in lithofacies LD3 is interpreted as glacimarine mud from meltwater, with the sand laminae deposited from down-slope gravity flows, e.g. turbidity currents (e.g. Gilbert, 1982; Elverhøi et al., 1983; Mackiewicz et al., 1984; Sexton et al., 1992; Ó Cofaigh & Dowdeswell, 2001). Where the sand and mud layers appear contorted, it likely relates to gravitational slump events that acted to rework and redeposit the sediments down-slope (e.g. Kuenen, 1948; Shanmugam et al., 1994; Forsberg et al., 1999). Turbidites are often associated with proximal glacimarine conditions (e.g. Gilbert, 1982;

Gilbert et al., 1993), suggesting that during the deposition of LD3 the margin of Jakobshavn Isbræ was relatively close. Although the turbidites could simply be a product of the abundant mass-flows occurring in Disko Bay due to the very irregular topography, an ice-proximal origin for LD3 is also supported by the radiocarbon dates, which provide evidence that LD3 was deposited around 9.2 cal ka BP in VC05, and between 7.8–7.7 ka BP in VC09 (the date of 8.1 ka BP in VC09 is considered unreliable, see section 4.3.2), during which time the ice margin was at or near Isfjeldsbanken (Lloyd et al., 2005; Long et al., 2006; Weidick & Bennike, 2007; Kelley et al., 2013). An ice-proximal origin for LD3 is further supported by the overall constant, relatively high MS, the close stratigraphic relationship of LD3 to the proximal sediments of LD2b (Fig. 6), and the lack of IRD, as large amounts of fresh glacial meltwater may have promoted debris retention in icebergs, or high SARs of mud may have swamped the input of IRD.

LD4 – stratified mud and diamict

The inter-stratified muds and diamicts of lithofacies LD4 are similar to deposits described from the continental shelf west of Disko Bay, which were linked to variations in meltwater-derived sediment flux, likely related to seasonal cycles (Hogan et al., 2016). As also argued by Hogan et al. (2016), such deposits can form in two ways: (1) the fine-grained layers form during summer, when IRD flux to the core sites is overwhelmed by increased influx of meltwater-derived fines. In winter, sedimentation from icebergs dominates over the reduced influx of fine-grained mud associated with lower melt rates, and the diamictic layers form (cf. Cowan et al., 1997; Hogan et al., 2016). (2) The fine-grained sediments are deposited during winter, when shore-fast sea ice traps icebergs and prevents the meltout and deposition of IRD, while subglacial meltwater delivers fine-grained mud to the core sites. In summer the sea ice breaks up and releases the icebergs, and their incorporated IRD melts out and forms the diamict layers (cf. Syvitski et al., 1996; Dowdeswell et al., 1998, 2000). The generally sharper upper boundaries of the diamict units in the lower parts of LD4 indicate an abrupt increase in meltwater discharge at the start of the summer season and/or increased sediment concentrations in the meltwater plumes (cf. Ó Cofaigh & Dowdeswell, 2001; Knudsen et al., 2007) and we thus suggest that the mud layers in LD4 were more likely deposited from a meltwater plume (cf. Hogan et al., 2016). The change to noticeably more diffuse boundaries towards the upper part of LD4 likely represents a transition from a more proximal glacimarine environment lower in LD4 to more distal conditions higher up in the facies (cf. Hogan et al., 2016). A radiocarbon date from LD4 indicates that this facies was deposited prior to 10.6 ka BP (Fig. 9), which supports this interpretation as the ice margin was probably slightly east of Isfjeldsbanken during this time (Lloyd et al., 2005). The date further provides an important constraint for the retreat of Jakobshavn Isbræ through Disko Bay (see section 5.2).

LD5 – pebbly mud

The muddy matrix in facies LD5 is interpreted as the product of hemipelagic or distal glacimarine suspension settling, with the predominantly angular clasts likely deposited from icebergs (cf. Dowdeswell & Dowdeswell, 1989). The high clast abundance points to (1) increased iceberg calving rates, (2) concentrated dumping events (i.e. overturning icebergs), (3) increased iceberg melt, or (4) a decreasing accumulation of fine-grained sediments from a retreating ice margin emphasising the IRD input (e.g. Elverhøi et al., 1980, 1983; Dowdeswell & Dowdeswell, 1989; Moros et al., 2002; Andresen et al., 2010; Seidenkrantz et al., 2013). The occurrence of LD5 in VC07 and VC09 does not seem to be linked to a specific climatic warming event, which suggests iceberg dumping to be the most likely cause of formation. Conversely, the deposition of LD5 dates to ~3.7 ka BP in VC05 during which time the Jakobshavn ice margin was located east of its present position (Weidick & Bennike, 2007). As some authors have suggested a late Holocene Thermal Maximum in Disko Bay and other West Greenland fjords lasting until at least ~3.5 ka BP (Moros et al., 2006; Møller et al., 2006; Seidenkrantz et al., 2007), the deposition of LD5 in this core could be linked to enhanced glacier and/or iceberg melting during the late stages of this climatic amelioration. As argued by Long & Roberts (2003), Roberts & Long (2005), and Lloyd (2006), warmer conditions would have led to reduced coupling between the glacier and its bed, and thus reduced supply of meltwater-derived fines to the core sites. The latter could be reflected in the low SARs (~0.02 cm a^{-1}) of LD5. Incidentally, although not specifically mentioned in the literature, such brief periods of climatic warming, or, alternatively, strengthened inflow of warm WGC waters, seem plausible in a system as climatically complex as Disko Bay and could thus also account for the occurrence of LD5 in VC07 and VC09. Notwithstanding this, the high concentration of IRD in LD5 could also imply a re-advance of Jakobshavn Isbræ, possibly related to the onset of Neoglaciation, which would have caused the ice to be subjected to the increasing influence of warm Atlantic water, leading to enhanced calving rates. The high flux of IRD would then have outpaced the flux of meltwater, leading to the deposition of a clast-rich mud. A higher iceberg availability was one of the reasons suggested for the high amounts of IRD in the lithological record from the Vaigat Strait (Andresen et al., 2010).

LV1 – massive mud with clasts

Based on its similarity to LD2a and sediments from the same area investigated by Andresen et al. (2010) and McCarthy (2011), we interpret LV1 from the Vaigat Strait as glacimarine mud deposited from meltwater plumes and/or the water column, and clasts settling from icebergs and sea ice drifting over the core sites. Large-scale re-working of the sediments down-slope into the Vaigat Strait probably led to the massive internal structure. The comparatively large number of clasts in LV1 can be explained by the fact, that, in addition to the icebergs from the local glaciers, icebergs calved from Jakobshavn Isbræ are also transported to the Vaigat Strait by the local ocean currents (Lloyd et al., 2005; Andresen et al., 2010; McCarthy, 2011).

5. Discussion

5.1. Landforms and sediment facies signature of Jakobshavn Isbræ and adjacent fast-flowing GIS outlets

The submarine landform assemblage in Disko Bay and the Vaigat Strait includes (1) streamlined bedrock ridges, (2) crag-and-tails, (3) submarine channels, and (4) pockmarks. TOPAS profiles further indicate the abundance of (5) deposits from gravitational mass-transport. The streamlined bedrock and crag-and-tails record the flow of an extended Jakobshavn Isbræ and adjacent GIS outlets across the bay during the LGM and are indicative of relatively fast ice flow (cf. King et al., 2009). The absence of recessional moraines, which are commonly observed in glaciated areas (e.g. Landvik, 1994; Ottesen et al., 2005; Ottesen & Dowdeswell, 2009; Dowdeswell et al., 2010; Hogan et al., 2010), suggests that retreat was so rapid that there was insufficient time for recessional moraines to form, or that retreat occurred as a floating ice shelf. An interpretation of rapid retreat is supported by the reconstructed high retreat rates from the continental shelf and from Disko Bay (discussed in section 5.3 below).

In terms of the Holocene sedimentary environments and the associated depositional processes in front of Jakobshavn Isbræ and adjacent GIS outlet glaciers, we identify four main processes: (1) suspension settling of glacimarine muds from meltwater and the water column, (2) meltout of coarser grains from icebergs and sea ice (3) sediment gravity flows, reworking both fine- and coarse-grained deposits down the slopes of submarine basins, and (4) ploughing of sediments by grounded iceberg keels. Meltwater-derived sedimentation is the dominant process, as indicated by the exceptionally well-sorted muds (usually $>95\%$ of the muds have a grain size $<63\ \mu$) and their overall strong terrestrial signal.

5.2. Timing of ice retreat and deglacial ice sheet dynamics

In order to reconstruct a retreat chronology for Jakobshavn Isbræ, we integrate the radiocarbon dates presented in this study with previously published data from both marine and terrestrial settings in West Greenland (Fig. 10). An extended Jakobshavn Isbræ and its adjacent GIS outlets flowed through Disko Bay and through the Vaigat Strait onto the continental shelf during the Last Glacial Maximum (cf. Ó Cofaigh et al., 2013; Dowdeswell et al., 2014). The ancestral Jakobshavn Isbræ commenced retreat from the outer continental shelf around 13.8 ka BP or before, and underwent a short-lived re-advance during the Younger Dryas on the shelf west of Disko Bay, at ~12.3–12.0 ka BP (re-calibrated from Ó Cofaigh et al., 2013). Deglaciation of the inner continental shelf and the western parts of Disko Bay was underway by 10.9 and 10.8 ka BP, respectively (Fig. 10; McCarthy, 2011; Hogan et al., 2012; Kelley et al., 2013). Our date of 10.6 ka BP from relatively proximal glacimarine sediments in central Disko Bay serves as a minimum age for deglaciation of the central bay and demonstrates that the ice margin had retreated to a position east of VC07 by this time. The 2.8 m-thick sequence of proximal sediments at the base of VC07 must have been deposited before this date and could indicate that the ice margin retreated very slowly (see also section 5.3 below) or paused close to the core site of VC07. A radiocarbon date published by Lloyd et al. (2005) from core POR18 showed that the ice margin was located at or somewhere within 6 km west of Isfjeldsbanken at 10.2 ka BP (re-calibrated; Fig. 10), and is in good agreement with findings from Young et al. (2011a), who place the ice margin at or close to Isfjeldsbanken at 10.2 ka BP. Sub-bottom profiler data presented by Hogan et al. (2011) suggest a prolonged still-stand of the ice margin at Isfjeldsbanken, which led to the accumulation of thick sedimentary basin infills immediately west of the sill. The radiocarbon dates from thick ice-proximal sedimentary sequences from inner Disko Bay (VC09 and VC05, this study; DA00-06, Lloyd et al., 2005; Hogan et al., 2011) further support this. Two re-advances of Jakobshavn Isbræ occurred in response to climatic cooling events around 9.3 and 8.2 ka BP (e.g. Young et al., 2013), the latter of which may be reflected in the transition from more distal (lithofacies LD2a) to more proximal glacimarine muds (LD2b) in VC09. The change from relatively proximal glacimarine (LD2b) to predominantly hemipelagic sediments (LD2c) in VC05 and VC09 implies that Jakobshavn Isbræ had retreated into Isfjorden sometime around 7.6–7.1 ka BP. This is consistent with work from Lloyd et al. (2005) and Hogan et al. (2011), who concluded that the ice stream retreated from Isfjeldsbanken into Isfjorden at c. 7.9–7.8 ka BP. Although Corbett et al. (2011) and Young et al. (2011b,a, 2013) suggested slightly earlier deglaciation of the coastal areas in eastern Disko Bay, it is possible that Jakobshavn Isbræ remained grounded at Isfjeldsbanken longer than the surrounding ice masses. During subsequent retreat the ice margin withdrew to a position behind that of the present terminus, where it remained throughout the mid-Holocene (Young et al., 2011a, 2013; Kelley et al., 2013), before it re-advanced westwards to its present position after 2.2 ka BP (cf. Weidick & Bennike, 2007).

In the Vaigat Strait, the chronology of deglaciation is less clear, reflecting a lack of data from this region but also the very thick post-glacial sediment cover, which makes it difficult to obtain radiocarbon ages relating to ice retreat through the strait. In fact, to our knowledge, the oldest date of 4.8 cal ka BP (re-calibrated) was obtained at a depth of 435 cm from a core from the central Vaigat Strait (Fig. 10; McCarthy, 2011), and is regarded as a minimum age for ice retreat.

5.3. Retreat rates

From the above constraints on the timing of ice retreat, minimum rates of retreat can be estimated for the ice sheet outlet glaciers, which retreated relatively quickly across the continental shelf, accelerated through Egedesminde Dyb, slowed slightly through western Disko Bay, and significantly slowed through the eastern bay. Note that the rates presented here are average rates, based on the assumption of linear ice retreat. The geomorphological and lithological

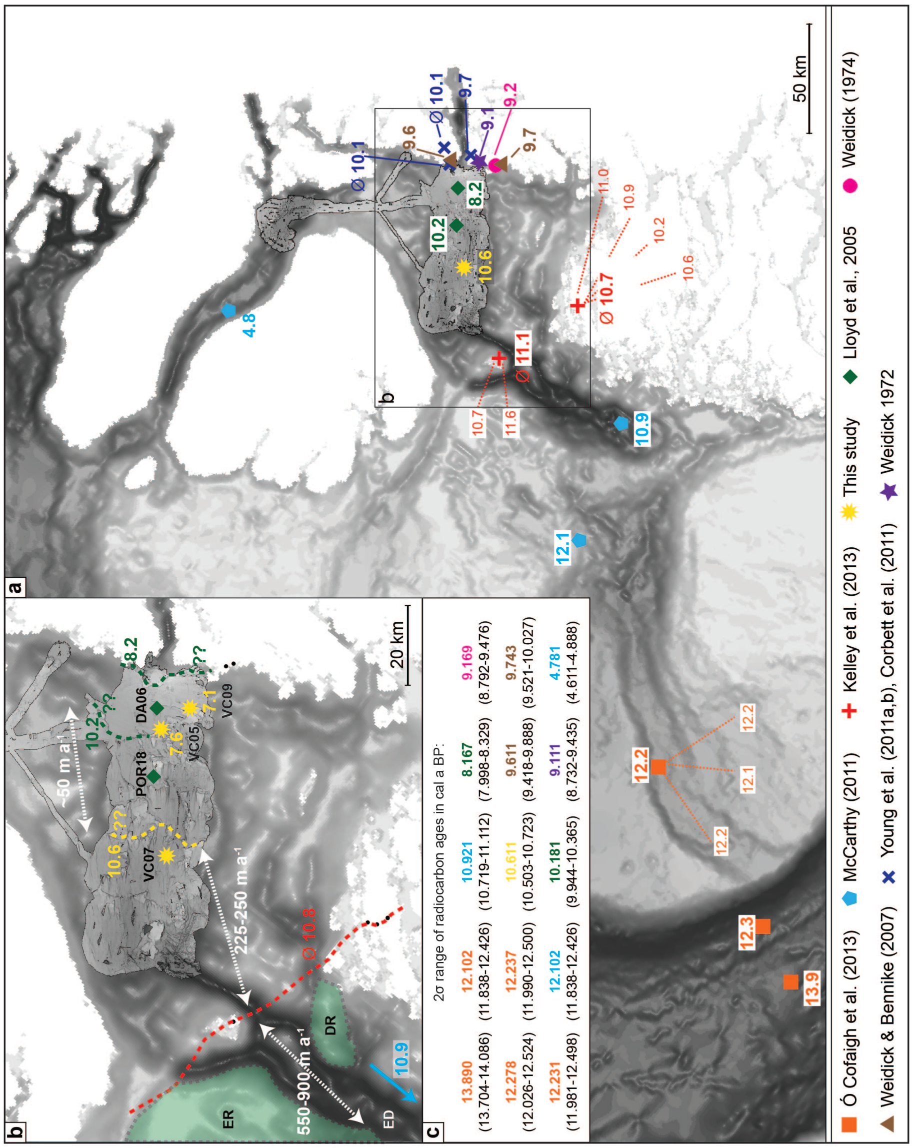
a
b
c
2σ range of radiocarbon ages in cal a BP:
13.890 (13.704-14.086)
12.102 (11.838-12.426)
10.921 (10.719-11.112)
8.167 (7.998-8.329)
9.169 (8.792-9.476)
12.278 (12.026-12.524)
12.237 (11.990-12.500)
10.611 (10.503-10.723)
9.611 (9.418-9.888)
9.743 (9.521-10.027)
12.231 (11.981-12.498)
12.102 (11.838-12.426)
10.181 (9.944-10.365)
9.111 (8.732-9.435)
4.781 (4.611-4.888)
550-900 m a-1
225-250 m a-1
~50 m a-1
ER
DR
ED
POR18
DA06
VC07
VC05
VC09
20 km
50 km
Ó Cofaigh et al. (2013)
McCarthy (2011)
Kelley et al. (2013)
This study
Lloyd et al., 2005
Weidick (1974)
Weidick & Bennike (2007)
Young et al. (2011a,b), Corbett et al. (2011)
Weidick 1972

evidence presented in this study suggests that the margin of Jakobshavn Isbræ was grounded during retreat. This is based on the implication of meltwater-dominated sedimentation with moderate input from icebergs and sea ice in the cores from Disko Bay and the Vaigat Strait, as sediment facies associated with ice shelves tend to be diamictic and coarse-grained close to the grounding line, and, in the case of the more distal sub-ice shelf sediments, tend to lack IRD (cf. e.g. Anderson et al., 1991; Powell et al., 1996; Domack et al., 1999; Kilfeather et al., 2011). Furthermore, the presence of a large submarine channel (C1, see section 4.1 and Figs. 3, 4) in the central bay is thought to support a grounded ice margin, because its depth, shape, and the close association with a transverse bedrock ridge seem consistent with subglacial meltwater excavation at the grounding line of a stagnating ice margin over an extended period of time. Nevertheless, the absence of recessional features on the seafloor in Disko Bay and the periodic appearance of coarse-grained diamicts (LD1 in VC03, VC04, and VC08) may reflect transient decoupling of the ice stream from its underlying bed. Indeed, a lightly grounded and relatively thin ice margin with predominantly hydrostatic support was already proposed by Hofmann et al. (2016), who further suggested that the ice stream may have grounded intermittently at bedrock highs. It is therefore possible, that, while our data mainly imply grounded ice, the ice stream experienced occasional periods of ungrounding, at

Figure 10 *(preceding page)*: a) Summary of radiocarbon (median) and ^{10}Be dates available from marine organisms on the continental shelf and Disko Bay, and from bedrock from adjacent land areas in (cal) ka BP. Radiocarbon dates from previously published studies were re-calibrated using a ΔR of 140±25 years (Lloyd et al., 2005). b) Zoom-in on the study area according to the rectangle indicated in a). Stippled red, yellow and green lines show an estimation of where the ice front position could have been based on the dates from boulders/bulk sediment (red; Kelley et al., 2013) and sediment cores (yellow for this study and green for Lloyd et al., 2005). White arrows and numbers imply possible retreat rates. Green shaded areas show Egedesminde Ridge (ER). ED = Egedesminde Dyb, DR = Disko Gneiss Ridge (cf. Hofmann et al., 2016). c) Summary of the 2σ ranges obtained from re-calibration of the radiocarbon ages.

least locally.

The ancestral Jakobshavn Isbræ retreated at rates between 22–275 m a^{-1} across the continental shelf after its Younger Dryas re-advance around 12.3–12.0 ka BP (Ó Cofaigh et al., 2013). A retreat of up to 90 km between c. 10.9 ka BP (re-calibrated radiocarbon date from McCarthy, 2011) and 10.8 ka BP (^{10}Be date from Kelley et al., 2013, Fig. 10) implies accelerated retreat through Egedesminde Dyb at rates between 550 and 900 m a^{-1}. Although these rates are much higher than those for the continental shelf, more extensive calving and thus faster ice retreat has often been linked to bathymetric overdeepening (e.g. Meier & Post, 1987; Seramur et al., 1997; Oerlemans & Nick, 2006; Benn et al., 2007; Ó Cofaigh, 1998; Kehrl et al., 2011). Furthermore, Egedesminde Ridge west of the trough (Fig. 10), could have served as a pinning point during ice retreat (Hofmann et al., 2016). Once the ice stream detached from this ridge, fast retreat would have occurred due to increased glacier bottom melting caused by the inflow of warm Atlantic water into the trough (cf. Andersen, 1981; Lloyd et al., 2005; Lloyd, 2006; Holland et al., 2008). The subsequent retreat across outer Disko Bay occurred over a minimum distance of 45 km between ∼10.8 and 10.6 ka BP to a position east of VC07, suggesting minimum rates between 225 and 250 m a^{-1} from the western to the central bay (Fig. 10). This shows that retreat either slowed, or that Jakobshavn Isbræ temporarily paused upon entering Disko Bay, which is likely, given the sudden shoaling from >1100 to 400 m water depth at the eastern end of Egedesminde Dyb and a sudden widening of the retreat basin (e.g. Oerlemans & Nick, 2006; Benn et al., 2007). Retreat was even slower through the eastern parts of the bay, as shown by dates of 10.6 ka BP from proximal glacimarine sediments in VC07 and 10.2 ka BP from similar sediments in POR18, which indicate a retreat of approximately 20 km at a rate of ∼50 m a^{-1} (Fig. 10; Lloyd et al., 2005, this study). Similar rates were obtained from the cosmogenic dates in the area, thus supporting slow or intermittent retreat through eastern Disko Bay (Kelley et al., 2013).

5.4. Comparison between West Greenland and other glacimarine environments

Suspension settling, ice rafting, sediment gravity flows, and iceberg ploughing were identified as the key sedimentary processes during deglaciation of Disko Bay and the Vaigat Strait. Although these four processes reflect those commonly observed in high-Arctic fjord environments (e.g. Elverhøi et al., 1983; Powell & Molnia, 1989; Andrews et al., 1994; Syvitski et al., 1996; Dowdeswell et al., 1998; Ó Cofaigh & Dowdeswell, 2001; Forwick et al., 2010), the variable magnitude of each of these has important implications for our understanding of glacimarine sedimentation. Thus far, depositional environments in front of tidewater glaciers have been categorised according to climatic and glaciological regime (Dowdeswell et al., 1998). Southeast Alaska forms the warmer end of the spectrum, with predominantly fine-grained mud deposited from glacial meltwater (Powell & Molnia, 1989; Cowan & Powell, 1991). Antarctica forms the other extreme, defined as a polar and climatically severe setting, where sedimentation occurs mainly at the grounding line (e.g. Domack et al., 1999; Powell et al., 1996; Ashley & Smith, 2000). Fjords around Svalbard and Baffin Island are in between these two end members (Dowdeswell et al., 1998) with high amounts of meltwater-derived muds close to the glacier fronts (e.g. Elverhøi et al., 1983; Gilbert, 1983; Gilbert et al., 1990; Forwick et al., 2010; Streuff et al., 2015), but increasing amounts of ice-rafted material towards ice-distal areas (e.g. Elverhøi et al., 1983; Forwick & Vorren, 2009; Kempf et al., 2013). East Greenland was initially defined as an environment with low meltwater availability, where sedimentation is dominated by iceberg-rafting and meltout from sea ice (e.g. Marienfeld, 1991; Syvitski et al., 1996; Dowdeswell et al., 1993, 1994, 1998). However, subsequent work by Smith & Andrews (2000) and Ó Cofaigh et al. (2001) showed that large amounts of fine-grained stratified sediments in proximal areas of East Greenland fjords record sedimentation predominantly from meltwater, and that deposition of IRD only becomes important in more ice-distal environments. Large amounts of silt and clay derived from meltwater were also observed in other East Greenland fjords (Andrews et al., 1994). Accordingly, Ó Cofaigh et al. (2001) proposed that glacimarine sedimentary processes can be very similar despite different climatic, glaciological and oceanographic settings, and that their variability may rather be a consequence, at least in part, of local controls, such as distance to the ice margin.

There has been limited research investigating glacimarine sedimentary processes in West Greenland and it has not been considered in the spectrum outlined above, perhaps due to the only recently emerging data (e.g. McCarthy, 2011; Jennings et al., 2013; Ó Cofaigh et al., 2013; Dowdeswell et al., 2014; Hogan et al., 2016; Sheldon et al., 2016). The abundance of meltwater-derived sediments in the cores from Disko Bay and the Vaigat Strait emphasise the importance of meltwater sedimentation in proximal areas of GIS outlets here and suggest that the ice-proximal sedimentary processes in West Greenland are comparable with those from warmer settings like Svalbard and Alaska (e.g. Powell & Molnia, 1989; Cowan & Powell, 1991; Cai et al., 1997; Forwick & Vorren, 2009; Forwick et al., 2010; Streuff et al., 2015). Considering the nearly identical mean annual air temperatures and annual precipitation between Svalbard and West Greenland and that both are influenced by relatively warm and saline Atlantic water, similar depositional processes may not be surprising. Similarity in sedimentary processes also suggests that in terms of depositional environment Disko Bay acts more like a fjord than a marine embayment on the continental shelf. However, the increasingly hemipelagic and diamictic sediments and the associated reduction in meltwater flux in the distal areas of Disko Bay (VC08 and VC07) are different from Svalbard and Alaska, where sedimentation from meltwater remains the dominant process throughout the entire glacimarine setting (Görlich et al., 1987; Boulton, 1990; Streuff et al., 2015). This strongly implies that glacimarine processes and their associated facies are not simply a function of climate. In fact, Disko Bay appears to be more similar to the glacimarine depositional environments of East Greenland fjords, which is notable given the classification of East Greenland as a polar, meltwater-restricted glacimarine environment, and the extensive sea ice in most of its fjords. The comparatively low SARs in Disko Bay with respect to those in East Greenland fjords may be related to differences in the availability of meltwater or glacial debris, or to the different fjord morphology compared to Spitsbergen and East Greenland fjords (wide open bay vs. narrow constricted fjords). It follows that even within geographically constrained areas glacimarine sedimentary processes and their magnitude can vary significantly over distance and time. We conclude that variability between meltwater-dominated and iceberg-dominated glacimarine sedimentation is not necessarily related only to climate and glaciology but is also dependent on local factors including distance to the ice margin, seafloor topography and glacier size (cf. Ó Cofaigh et al., 2001).

6. Conclusions

Lithological data integrated with swath bathymetry and TOPAS sub-bottom profiler data provide new insights into the Holocene glacimarine sedimentary processes in Disko Bay and the Vaigat Strait in West Greenland. Vibrocores comprise diamict, (diffusely) stratified mud, massive mud with sharp-based sand layers, IRD-rich massive mud, and massive bioturbated muds. These facies show that suspension settling of fine-grained sediment from turbid meltwater plumes and the water column, sediment gravity flows, and iceberg rafting and ploughing were the dominant sedimentary processes during and following ice retreat, with meltwater sedimentation dominant in ice-proximal areas, and hemipelagic suspension settling and IRD-rainout from icebergs dominant in distal areas.

Our findings show that despite similar climate and oceanography glacimarine sedimentary processes differ between Svalbard and West Greenland, but are similar between East and West Greenland in spite of different oceanographic conditions. This confirms that such processes vary more as a function of local controls such as distance from the ice margin and geomorphological setting rather than climate and geographic location. Radiocarbon dates provide the basis for estimated SARs between 0.1 and 1.7 cm a^{-1} in proximal areas, and $\sim$0.007–0.05 cm a^{-1} in distal areas, which are lower than SARs documented for

East Greenland. The radiocarbon dates further constrain the retreat dynamics of Jakobshavn Isbræ during deglaciation. Streamlined glacial landforms, including crag-and-tails and glacial lineations, record the former flow of an expanded Jakobshavn Isbræ and adjacent GIS outlets through Disko Bay and the Vaigat Strait towards the adjoining continental shelf. During deglaciation, retreat was relatively fast across the continental shelf (22–250 m a^{-1}), through Egedesminde Dyb ($\sim$550–900 m a^{-1}), and the western parts of Disko Bay ($\sim$225–250 m a^{-1}), all of which were deglaciated before 10.6 ka BP. Subsequent retreat through eastern Disko Bay was much slower ($\sim$50 m a^{-1}), and likely interrupted by at least one still-stand due to pinning of the grounded glacier margin on submarine bedrock ridges. The ice margin paused again at Isfjeldsbanken before retreating into Isfjorden. Around 7.6–7.1 ka BP the ice margin had probably retreated far back into Isfjorden, as at this point sediment delivery to the core sites from meltwater plumes became significantly reduced. The variable retreat rates and sedimentary facies we document here underscore the importance of local morphology and glacier proximity for the palaeo-retreat dynamics and associated glacimarine sedimentary processes of marine-terminating Greenland Ice Sheet outlet glaciers.

Acknowledgements

This research has received funding from the UK Natural Environment Research Council (Grants NE/D001986/1 and NE/ D001951/1) and the People Programme (Marie Curie Actions) of the European Union's Seventh Framework Programme FP7/2007-2013/ under REA grant agreement no. 317217. Some of the radiocarbon dates were acquired with the NSF-OPP-0713755 grant awarded to Anne Jennings by the National Science Foundation, USA. We thank the participants and crew of the JR175 research cruise for their help with data acquisition. Neil Tunstall and Frank Davies kindly assisted with the use of the MSCL. Discussions with Elena Grimoldi, Louise Callard and Kasper Weilbach and the comments from two anonymous reviewers further helped to improve the

manuscript.

References

Alley, R., Clark, P., Huybrechts, P., & Joughin, I. (2005). Ice-sheet and sea-level changes. *Science*, *310*, 456–60. doi:10.1126/science.1114613.

Andersen, O. (1981). The annual cycle of temperature, salinity, currents and water masses in Disko Bugt and adjacent waters, West Greenland. *Meddelelser on Grønland, Bioscience*, *5*.

Anderson, J., Kennedy, D., Smith, M., & Domack, E. (1991). Sedimentary facies associated with Antarcticas floating ice masses. *Geological Society of America Special Papers*, *261*, 1–26. doi:10.1130/SPE261-p1.

Andresen, C., McCarthy, D., Dylmer, C., Seidenkrantz, M., Kuijpers, A., & Lloyd, J. (2010). Interaction between subsurface ocean waters and calving of the Jakobshavn Isbræ during the late Holocene. *The Holocene*, (pp. 1–14). doi:10.1177/0959683610378877.

Andrews, J., Milliman, J., Jennings, A., Rynes, N., & Dwyer, J. (1994). Sediment thicknesses and Holocene glacial marine sedimentation rates in three east Greenland fjords (ca. 68° N). *The Journal of Geology*, *102*, 669–83. doi:10.1086/629711.

Ashley, G., & Smith, N. (2000). Marine sedimentation at a calving glacier margin. *The Geological Society of America Bulletin*, *112*, 657–67. doi:10.1130/0016.

Bamber, J., Alley, R., & Joughin, I. (2007). Rapid response of modern day ice sheets to external forcing. *Earth and Planetary Science Letters*, *257*, 1–13. doi:doi:10.1016/j.epsl.2007.03.005.

Benn, D., Warren, C., & Mottram, R. (2007). Calving processes and the dynamics of calving glaciers. *Earth-Science Reviews*, *82*, 143–79. doi:10.1016/j.earscirev.2007.02.002.

Bennike, O. (2000). Palaeoecological studies of Holocene lake sediments from west Greenland. *Palaeogeography, Palaeoclimatology, Palaeoecology*, *155*, 285–304. doi:10.1016/S0031-0182(99)00121-2.

Bindschadler, R. (1984). Jakobshavns Glacier drainage basin: a balance assessment. *Journal of Geophysical Research: Oceans*, *89*, 2066–72. doi:10.1029/JC089iC02p02066.

Boulton, G. (1990). Sedimentary and sea level changes during glacial cycles and their control on glacimarine facies architecture. *Geological Society, London, Special Publications*, *53*, 15–52. doi:10.1144/GSL.SP.1990.053.01.02.

Cai, J., Powell, R., Cowan, E., & P., C. (1997). Lithofacies and seismic-reflection interpretation of temperate glacimarine sedimentation in Tarr Inlet, Glacier Bay, Alaska. *Marine Geology*, *143*, 5–37. doi:10.1016/S0025-3227(97)00088-1.

Caress, D. W., & Chayes, D. N. (1996). Improved processing of Hydrosweep DS multibeam data on the R/V Maurice Ewing. *Marine Geophysical Research*, *18*, 631–50. doi:10.1007/BF00313878.

Chalmers, J., Pulvertaft, T., Marcussen, C., & Pedersen, A. (1999). New insight into the structure of the Nuussuaq Basin, central West Greenland. *Marine and Petroleum Geology*, *16*, 197–224. doi:doi:10.1016/S0264-8172(98)00077-4.

Corbett, L., Young, N., Bierman, P., Briner, J., Neumann, T., Rood, D., & Graly, J. (2011). Paired bedrock and boulder ^{10} Be concentrations resulting from early Holocene ice retreat near Jakobshavn Isfjord, western Greenland. *Quaternary Science Reviews*, *30*, 1739–49. doi:10.3198/1996JoG42-141-219-232.

Cowan, E., Cai, J., Powell, R., Clark, J., & Pitcher, J. (1997). Temperate glacimarine varves: an example from Disenchantment Bay, southern Alaska. *Journal of Sedimentary Research*, *67*, 536–49.

Cowan, E., & Powell, R. (1991). Ice-proximal sediment accumulation rates in a temperate glacial fjord, southeastern Alaska. *Geological Society of America Special Papers*, *261*, 61–74. doi:10.1130/SPE261-p61.

Dionne, J. (1987). Tadpole rock (rocdrumlin): a glacial streamline moulded form. In *Drumlin Symposium. Rotterdam: Balkema* (p. 159). volume 149.

Domack, E., Jacobson, E., Shipp, S., & Anderson, J. (1999). Late Pleistocene–Holocene retreat of the West Antarctic Ice-Sheet system in the Ross Sea: Part 2 – sedimentologic and stratigraphic signature. *Geological Society of America Bulletin*, *111*, 1517–36. doi:10.1130/0016-7606(1999)111.

Domack, E. W. (1984). Rhythmically bedded glaciomarine sediments on Whidbey Island, Washington. *Journal of Sedimentary Research*, *54*.

Dowdeswell, J. A., & Dowdeswell, E. (1989). Debris in Icebergs and Rates of Glaci-Marine Sedimentation: Observations from Spitsbergen and a Simple Model. *The Journal of Geology*, *97*, 221–31. doi:10.1086/629296.

Dowdeswell, J. A., Dowdeswell, E., & Rodrigo, C. (2016). Pockmarks in the fjords of Chilean Patagonia. In J. A. Dowdeswell, M. Canals, M. Jakobsson, B. J. Todd, E. K. Dowdeswell, & K. A. Hogan (Eds.), *Atlas of submarine glacial landforms* number 46 in Geological Society Memoir (pp. 109–10). The Geological Society London. doi:10.1144/M46.159.

Dowdeswell, J. A., Elverhøi, A., & Spielhagen, R. (1998). Glacimarine sedimentary processes and facies on the Polar North Atlantic margins. *Quaternary Science Reviews*, *17*, 243–72. doi:10.1016/S0277-3791(97)00071-1.

Dowdeswell, J. A., Hogan, K., Evans, J., Noormets, R., Ó Cofaigh, C., & Ottesen, D. (2010). Past ice-sheet flow east of Svalbard inferred from streamlined subglacial landforms. *Geology*, *38*, 163–6. doi:10.1130/G30621.1.

Dowdeswell, J. A., Hogan, K., Ó Cofaigh, C., Fugelli, E., Evans, J., & Noormets, R. (2014). Late Quaternary ice flow in a West Greenland fjord and cross-shelf trough system: submarine landforms from Rink Isbrae to Uummannaq shelf and slope. *Quaternary Science Reviews*, *92*, 292–309. doi:10.1016/j.quascirev.2013.09.007.

Dowdeswell, J. A., Villinger, H., Whittington, R. J., & Marienfeld, P. (1993). Iceberg scouring in Scoresby Sund and on the East Greenland continental shelf. *Marine Geology*, *111*, 37–53. doi:10.1111/j.1502-3885.1994.tb00602.x.

Dowdeswell, J. A., Whittington, R., Jennings, A., Andrews, J., Mackensen, A., & Marienfeld, P. (2000). An origin for laminated glacimarine sediments through sea-ice build-up and suppressed iceberg rafting. *Sedimentology*, *47*. doi:10.1046/j.1365-3091.2000.00306.x.

Dowdeswell, J. A., Whittington, R., & Marienfeld, P. (1994). The origin of massive diamicton facies by iceberg rafting and scouring, Scoresby Sund, East Greenland. *Sedimentology*, *41*, 21–35. doi:10.1111/j.1365-3091.1994.tb01390.x.

Echelmeyer, K., Clarke, T., & Harrison, W. (1991). Surficial glaciology of Jakobshavns Isbræ, West Greenland: Part I: Surface morphology. *Journal of Glaciology*, *37*, 368–82. doi:10.3198/1991JoG37-127-368-382.

Elverhøi, A., Liestøl, O., & Nagy, J. (1980). Glacial erosion, sedimentation and microfauna in the inner part of Kongsfjorden, Spitsbergen. *Norsk Polarinstitutt Skrifter*, *172*, 33–58.

Elverhøi, A., Lønne, Ø., & Seland, R. (1983). Glaciomarine sedimentation in a modern fjord environment, Spitsbergen. *Polar Research*, *1*, 127–50. doi:10.1111/j.1751-8369.1983.tb00697.x.

Flink, A. E., Noormets, R., Kirchner, N., Benn, D. I., Luckman, A., & Lovell, H. (2015). The evolution of a submarine landform record following recent and multiple surges of Tunabreen glacier, Svalbard. *Quaternary Science Reviews*, *108*, 37–50. doi:10.1016/j.quascirev.2014.11.006.

Forsberg, C. F., Solheim, A., Elverhøi, A., Jansen, E., Channell, J., & Andersen, E. S. (1999). The depositional environment of the western Svalbard margin during the Late Pliocene and the Pleistocene: Sedimentary facies changes at Site 9. In *Proceedings of the Ocean Drilling Program: Scientific results* (p. 233). The Program volume 162.

Forwick, M., Baeten, N., & Vorren, T. (2009). Pockmarks in Spitsbergen fjords. *Norwegian Journal of Geology*, *89*, 65–77.

Forwick, M., & Vorren, T. (2009). Late Weichselian and Holocene sedimentary environments and ice rafting in Isfjorden, Spitsbergen. *Paleogeography, Paleoclimatology, Paleoecology*, *280(1)*, 258–74. doi:10.1016/j.palaeo.2009.06.026.

Forwick, M., & Vorren, T. (2011). Stratigraphy and deglaciation of the Isfjorden area, Spitsbergen. *Norwegian Journal of Geology*, *90*, 163–79.

Forwick, M., Vorren, T., Hald, M., Korsun, S., Roh, Y., Vogt, C., & Yoo, K. (2010). Spatial and temporal influence of glaciers and rivers on the sedimentary environment in Sassenfjorden and Tempelfjorden, Spitsbergen. *Geological Society, London, Special Publications*, *344(1)*, 163–93. doi:10.1144/SP344.13.

Forwick, M., & Vorren, T. O. (2012). Submarine Mass Wasting in Isfjorden, Spitsbergen. In Y. Yamada, K. Kawamura, K. Ikehara, Y. Ogawa, R. Urgeles, D. Mosher, J. Chaytor, & M. Strasser (Eds.), *Submarine mass movements and their consequences* (pp. 711–22). Springer Springer+ Business Media volume 31. doi:10.1007/978-94-007-2162-3_63.

Funder, S., & Hansen, L. (1996). *The Greenland ice sheet – a model for its culmination and decay during and after the Last Glacial Maximum*. Geological Society of Denmark.

Funder, S., Kjellerup, K., Kjær, K., & Ó Cofaigh, C. (2011). The Greenland ice sheet during the past 300,000 years: a review. *Quaternary Glaciations - Extent and Chronology. Part IV: A closer look.: Developments in Quaternary Science*, *15*, 699–713. doi:10.1016/B978-0-444-53447-7.00050-7.

Gilbert, R. (1982). Contemporary sedimentary environments on Baffin Island, NWT, Canada: Glaciomarine processes in fiords of eastern Cumberland Peninsula. *Arctic and Alpine Research*, *14*, 1–12. doi:10.2307/1550809.

Gilbert, R. (1983). Sedimentary processes of Canadian Arctic fjords. *Sedimentary Geology*, *36(2–4)*, 147–75. doi:10.1016/0037-0738(83)90007-6.

Gilbert, R., Aitken, A., & Lemmen, D. (1993). The glacimarine sedimentary environment of Expedition Fiord, Canadian High Arctic. *Marine Geology*, *110*, 257–73. doi:10.1016/0025-3227(93)90088-D.

Gilbert, R., Naldrett, D. L., & Horvath, V. (1990). Holocene sedimentary environment of Cambridge Fiord, Baffin Island, Northwest Territories. *Sedimentology of Arctic Fiords*, *27*, 271–80. doi:10.1139/e90-026.

Gilbert, R., Nielsen, N., Möller, H., Desloges, J., & Rasch, M. (2002). Glacimarine sedimentation in Kangerdluk (Disko Fjord), West Greenland, in response to a surging glacier. *Marine Geology*, *191*, 1–18. doi:10.1016/S0025-3227(02)00543-1.

Görlich, K., Westawski, J., & Zajaczkowski, M. (1987). Suspension settling effect on macrobenthos biomass distribution in the Hornsund fjord, Spitsbergen. *Polar Research*, *5*, 175–92. doi:10.1111/j.1751-8369.1987.tb00621.x.

Grobe, H. (1987). A simple method for the determination of ice-rafted debris in sediment cores. *Polarforschung*, *57 (3)*, 123–6.

Harrington, P. (1985). Formation of pockmarks by pore-water escape. *Geo-Marine Letters*, *5*, 193–7. doi:10.1007/BF02281638.

Hofmann, J., Knutz, P., Nielsen, T., & Kuijpers, A. (2016). Seismic architecture and evolution of the Disko Bay trough-mouth fan, central West Greenland margin. *Quaternary Science Reviews*, *147*, 69–90. doi:10.1016/j.quascirev.2016.05.019.

Hogan, K., Dix, J., Lloyd, J., Long, A., & Cotterill, C. (2011). Seismic stratigraphy records the deglacial history of Jakobshavn Isbræ, West Greenland. *Journal of Quaternary Science*, *26(7)*, 757–66. doi:10.1002/jqs.1500.

Hogan, K., Dowdeswell, J., & Ó Cofaigh, C. (2012). Glacimarine sedimentary processes and depositional environments in an embayment fed by West Greenland ice streams. *Marine Geology*, *311*, 1–16. doi:10.1016/j.margeo.2012.04.006.

Hogan, K., Ó Cofaigh, C., Jennings, A., Dowdeswell, J., & Hiemstra, J. (2016). Deglaciation of a major palaeo-ice stream in Disko Trough, West Greenland. *Quaternary Science Reviews*, *147*, 5–26. doi:10.1016/j.quascirev.2016.01.018.

Hogan, K. A., Dowdeswell, J. A., Noormets, R., Evans, J., & Ó Cofaigh, C. (2010). Evidence for full-glacial flow and retreat of the Late Weichselian Ice Sheet from the waters around Kong Karls Land, eastern Svalbard. *Quaternary Science Reviews*, *29*, 3563–82. doi:10.1016/j.quascirev.2010.05.026.

Holland, D., Thomas, R., De Young, B., Ribergaard, M., & Lyberth, B. (2008). Acceleration of Jakobshavn Isbræ triggered by warm subsurface ocean waters. *Nature Geoscience*, *1*, 659–64. doi:10.1038/ngeo316.

Hovland, M., & Judd, A. G. (1988). *Seabed pockmarks and seepages: impact on geology, biology and the marine environment*.

Howat, I., Ahn, Y., Joughin, I., Van Den Broeke, M., Lenaerts, J., & Smith, B. (2011). Mass balance of Greenland's three largest outlet glaciers, 2000–2010. *Geophysical Research Letters*, *38*. doi:DOI: 10.1029/2011GL047565.

Hunt, A. G., & Malin, P. E. (1998). Possible triggering of heinrich events by ice-load-induced earthquakes. *Nature*, *393*, 155–8. doi:10.1038/30218.

Jennings, A., Walton, M., Ó Cofaigh, C., Kilfeather, A., Andrews, J., Ortiz, J., De Vernal, A., & Dowdeswell, J. (2013). Paleoenvironments during Younger Dryas – Early Holocene retreat of the Greenland Ice Sheet from outer Disko

Trough, central west Greenland. *Journal of Quaternary Science*, *2652*, 1–14. doi:10.1002/jqs.2652.

Joughin, I., Abdalati, W., & Fahnestock, M. (2004). Large fluctuations in speed on Greenland's Jakobshavn Isbrae glacier. *Nature*, *432*, 608–10. doi:10.1038/nature03130.

Joughin, I., Smith, B., Shean, D., & Floricioiu, D. (2014). Brief Communication: Further summer speedup of Jakobshavn Isbræ. *The Cryosphere*, *8*, 209–14. doi:10.5194/tc-8-209-2014.

Kehrl, L., Hawley, R., Powell, R., & Brigham-Grette, J. (2011). Glacimarine sedimentation processes at Kronebreen and Kongsvegen, Svalbard. *Journal of Glaciology*, *57(205)*, 841–7. doi:10.3189/002214311798043708.

Kelley, S., Briner, J., & Young, N. (2013). Rapid ice retreat in Disko Bugt supported by ^{10}Be dating of the last recession of the western Greenland Ice Sheet. *Quaternary Science Reviews*, *82*, 13–22. doi:10.1016/j.quascirev.2013.09.018.

Kempf, P., Forwick, M., Laberg, J., & Vorren, T. (2013). Late Weichselian – Holocene sedimentary palaeoenvironment and glacial activity in the high-Arctic van Keulenfjorden, Spitsbergen. *The Holocene*, *23(11)*, 1607–18. doi:10.1177/0959683613499055.

Kilfeather, A., Ó Cofaigh, C., Lloyd, J., Dowdeswell, J., Xu, S., & Moreton, S. (2011). Ice-stream retreat and ice-shelf history in Marguerite Trough, Antarctic Peninsula: Sedimentological and foraminiferal signatures. *Geological Society of America Bulletin*, *123*, 997–1015. doi:10.1130/B30282.1.

King, E., Hindmarsh, R., & Stokes, C. (2009). Formation of mega-scale glacial lineations observed beneath a West Antarctic ice stream. *Nature Geoscience*, *2(8)*, 585–8. doi:10.1038/ngeo581.

Knudsen, N., Yde, J., & Gasser, G. (2007). Suspended sediment transport in glacial meltwater during the initial quiescent phase after a major surge event at Kuannersuit Glacier, Greenland. *Geografisk Tidsskrift-Danish Journal of Geography*, *107*, 1–7. doi:DOI:10.1080/00167223.2007.10801370.

Kuenen, P. (1948). Slumping in the Carboniferous rocks of Pembrokeshire. *Quarterly Journal of the Geological Society*, *104*, 365–85. doi:10.1144/GSL.JGS.1948.104.01-04.18.

Landvik, J. (1994). The last glaciation of Germania Land and adjacent areas, northeast Greenland. *Journal of Quaternary Science*, *9*, 81–92. doi:10.1002/jqs.3390090108.

Lane, T. P., Roberts, D. H., Rea, B. R., Ó Cofaigh, C., Vieli, A., & Rodés, A. (2014). Controls upon the Last Glacial maximum deglaciation of the northern Uummannaq ice stream system, West Greenland. *Quaternary Science Reviews*, *92*, 324–44. doi:10.1016/j.quascirev.2013.09.013.

Larsen, J., & Pulvertaft, T. (2000). *The structure of the Cretaceous-Palaeogene sedimentary-volcanic area of Svartenhuk Halvø, central West Greenland* volume 188. Geological Survey of Denmark and Greenland, Ministry of Environment and Energy.

Linch, L. D., & Dowdeswell, J. A. (2016). Micromorphology of diamicton affected by iceberg-keel scouring, Scoresby Sund, East Greenland. *Quaternary Science Reviews*, *152*, 169–96. doi:10.1016/j.quascirev.2016.09.013.

Lloyd, J. (2006). Late Holocene environmental change in Disko Bugt, west Greenland: interaction between climate, ocean circulation and Jakobshavn Isbrae. *Boreas*, *35*, 35–49. doi:10.1111/j.1502-3885.2006.tb01111.x.

Lloyd, J., Moros, M., Perner, K., Telford, R., Kuijpers, A., Jansen, E., & McCarthy, D. (2011). A 100 yr record of ocean temperature control on the stability of Jakobshavn Isbrae, West Greenland. *Geology*, *39(9)*, 867–70. doi:10.1130/G32076.1.

Lloyd, J., Park, L., Kuijpers, A., & Moros, M. (2005). Early Holocene palaeoceanography and deglacial chronology of Disko Bugt, West Greenland. *Quaternary Science Reviews*, *24*, 1741–55. doi:10.1111/j.1502-3885.2006.tb01111.x.

Long, A., & Roberts, D. (2003). Late Weichselian deglacial history of Disko Bugt, West Greenland, and the dynamics of the Jakobshavns Isbrae ice stream. *Boreas*, *32*, 208–26. doi:10.1111/j.1502-3885.2003.tb01438.x.

Long, A., Roberts, D., & Dawson, S. (2006). Early Holocene history of the west Greenland Ice Sheet and the GH-8.2 event. *Quaternary Science Reviews*, *25*, 904–22. doi:10.1016/j.quascirev.2005.07.002.

Mackiewicz, N., Powell, R., Carlson, P., & Molnia, B. (1984). Interlaminated ice-proximal glacimarine sediments in Muir Inlet, Alaska. *Marine Geology*, *57*, 113–47. doi:10.1016/0025-3227(84)90197-X.

Marienfeld, P. (1991). Holozäne Sedimentationsentwicklung im Scoresby Sund, Ost–Grönland, . *96*, 162.

Marienfeld, P. (1992). Postglacial sedimentary history of Scoresby Sund, East Greenland. *Polarforschung*, *60*, 181–95.

McCarthy, D. (2011). *Late Quaternary ice-ocean interactions in central West Greenland*. Ph.D. thesis Department of Geography, University of Durham, UK.

Meier, M., & Post, A. (1987). Fast tidewater glaciers. *Journal of Geophysical Research: Solid Earth*, *92*, 9051–8. doi:10.1029/JB092iB09p09051.

Møller, H., Jensen, K., Kuijpers, A., Aagaard-Sørensen, S., Seidenkrantz, M.-S., Prins, M., Endler, R., & Mikkelsen, N. (2006). Late-Holocene environment and climatic changes in Ameralik Fjord, southwest Greenland: evidence from the sedimentary record. *The Holocene*, *16*, 685–95. doi:10.1191/0959683606hl963rp.

Moon, T., & Joughin, I. (2008). Changes in ice front position on Greenland's outlet glaciers from 1992 to 2007. *Journal of Geophysical Research: Earth Surface*, *113*. doi:10.1029/2007JF000927.

Moros, M., Jensen, K., & Kuijpers, A. (2006). Mid-to late-Holocene hydrological and climatic variability in Disko Bugt, central West Greenland. *The Holocene*, *16*, 357–67. doi:10.1191/0959683606hl933rp.

Moros, M., Kuijpers, A., Snowball, I., Lassen, S., Bäckström, D., Gingele, F., & McManus, J. (2002). Were glacial iceberg surges in the North Atlantic triggered by climatic warming? *Marine Geology*, *192*, 393–417. doi:doi:10.1016/S0025-3227(02)00592-3.

Nick, F., Vieli, A., Howat, I., & Joughin, I. (2009). Large-scale changes in Greenland outlet glacier dynamics triggered at the terminus. *Nature Geoscience*, *2*, 110–4. doi:doi:10.1038/ngeo394.

Nielsen, T., Laier, T., Kuijpers, A., Rasmussen, T., Mikkelsen, N., & Nørgård-Pedersen, N. (2014). Fluid flow and methane ooccurrence in the Disko Bugt area offshore West Greenland: indications for gas hydrates? *Geo-Marine Letters*, *34*, 511–23. doi:DOI 10.1007/s00367-014-0382-2.

Ó Cofaigh, C. (1998). Geomorphic and sedimentary signatures of early Holocene deglaciation in High Arctic fiords, Ellesmere Island, Canada: implications for deglacial ice dynamics and thermal regime. *Canadian Journal of Earth Sciences*, *35*, 437–52. doi:10.1139/e97-116.

Ó Cofaigh, C., & Dowdeswell, J. (2001). Laminated sediments in glacimarine environments: diagnostic criteria for their interpretation. *Quaternary Science Reviews*, *20*, 1411–36. doi:10.1016/S0277-3791(00)00177-3.

Ó Cofaigh, C., Dowdeswell, J., Allen, C., Hiemstra, J., Pudsey, C., Evans, J., & Evans, D. (2005). Flow dynamics and till genesis associated with a marine-based Antarctic paleo-ice stream. *Quaternary Science Reviews*, *24*, 709–40. doi:10.1016/j.quascirev.2004.10.006.

Ó Cofaigh, C., Dowdeswell, J., & Grobe, H. (2001). Holocene glacimarine sedimentation, inner Scoresby Sund, East Greenland: the influence of fast-flowing ice-sheet outlet glaciers. *Marine Geology*, *175*, 103–29. doi:10.1016/S0025-3227(01)00117-7.

Ó Cofaigh, C., Dowdeswell, J., Jennings, A., Hogan, K., Kilfeather, A., Hiemstra, J., Noormets, R., Evans, J., McCarthy, D., Andrews, J., Lloyd, J., & Moros, M. (2013). An extensive and dynamic ice sheet on the West Greenland shelf during the last glacial cycle. *Geology*, *41*, 219–22. doi:10.1130/G33759.1.

Oerlemans, J., & Nick, F. (2006). Modelling the advance–retreat cycle of a tidewater glacier with simple sediment dynamics. *Global and Planetary Change*, *50*, 148–60. doi:10.3189/172756407782871440.

Ottesen, D., & Dowdeswell, J. (2006). Assemblages of submarine landforms produced by tidewater glaciers in Svalbard. *Journal of Geophysical Research*, *111*, F01016. doi:10.1029/2005JF000330.

Ottesen, D., & Dowdeswell, J. (2009). An inter-ice stream glaciated margin: submarine landforms and a geomorphic model based on marine-geophysical data from Svalbard. *Geological Society of America Bulletin*, *121(11/12)*, 1647–65. doi:10.1130/B26467.1.

Ottesen, D., Dowdeswell, J., Benn, D., Kristensen, L., Christiansen, H., Christensen, O., & Vorren, T. (2008). Submarine landforms characteristic of glacier surges in two Spitsbergen fjords. *Quaternary Science Reviews*, *27(15)*, 1583–99. doi:10.1016/j.quascirev.2008.05.007.

Ottesen, D., Dowdeswell, J., & Rise, L. (2005). Submarine landforms and the reconstruction of fast-flowing ice streams within a large Quaternary ice sheet: the 2500-km-long Norwegian-Svalbard margin (57°– 80°N). *Geological Society of America Bulletin*, *117*, 1033–50. doi:10.1130/B25577.1.

Perner, K., Moros, M., Snowball, I., Lloyd, J., Kuijpers, A., & Richter, T. (2013). Establishment of modern circulation patterns at c. 6000 cal a BP in Disko Bugt, central West Greenland: Opening of the Vaigat Strait. *Journal of Quaternary Science*, *28*, 480–9. doi:10.1002/jqs.2638.

Powell, R., Dawber, M., McInnes, J., & Pyne, A. (1996). Observations of the grounding-line area at a floating glacier terminus. *Annals of Glaciology*, *22*, 217–23. doi:10.3198/1996AoG22-1-217-223.

Powell, R., & Molnia, B. (1989). Glacimarine sedimentary processes, facies and morphology of the south-southeast Alaska shelf and fjords. *Marine Geology*, *85*, 359–90. doi:10.1016/0025-3227(89)90160-6.

Rasch, M. (2000). Holocene relative sea-level changes in Disko Bugt, West Greenland. *Journal of Coastal Research*, *16*, 306–15. URL: http://www.jstor.org/stable/4300039.

Reimer, P., Bard, E., Bayliss, A., Beck, J., Blackwell, P., Ramsey, C., Buck, C., Cheng, H., Edwards, R., Friedrich, M., Grootes, P., Guilderson, T., Haflidason, H., Hajdas, I., Hatté, C., Heaton, T., Hoffmann, D., Hogg, A., Hughen, K., Kaiser, F., Kromer, B., Manning, S., Niu, M., Reimer, R., Richards, D., Scott, E., Southon, J., Staff, R., Turney, C., & van der Plicht, J. (2013). IntCal13 and Marine13 Radiocarbon Age Calibration Curves 0–50,000 Years cal BP. *Radiocarbon*, *55*, 1869–87. doi:10.2458/azu_js_rc.55.16947.

Ribergaard, M., & Buch, E. (2008). Oceanographic investigations off west Greenland 2007. *NAFO Scientific Council Documents*, *7*.

Rignot, E., & Kanagaratnam, P. (2006). Changes in the velocity structure of the Greenland Ice Sheet. *Science*, *311*, 986–90. doi:DOI: 10.1126/science.1121381.

Rignot, E., Koppes, M., & Velicogna, I. (2010). Rapid submarine melting of the calving faces of West Greenland glaciers. *Nature Geoscience*, *3*, 187–91. doi:10.1038/ngeo765.

Rinterknecht, V., Gorokhovich, Y., Schaefer, J., & Caffee, M. (2009). Preliminary ^{10}Be chronology for the last deglaciation of the western margin of the Greenland Ice Sheet. *Journal of Quaternary Science*, *24*, 270–8. doi:10.1002/jqs.1226.

Roberts, D., & Long, A. (2005). Streamlined bedrock terrain and fast ice flow, Jakobshavns Isbrae, West Greenland: implications for ice stream and ice sheet dynamics. *Boreas*, *34*, 25–42. doi:DOI: 10.1111/j.1502-3885.2005.tb01002.x.

Robinson, S. (1993). Lithostratigraphic applications for magnetic susceptibility logging of deep-sea sediment cores: examples from ODP Leg 115. *Geological Society, London, Special Publications*, *70*, 65–98. doi:10.1144/GSL.SP.1993.070.01.06.

Schumann, K., Völker, D., & Weinrebe, W. (2012). Acoustic mapping of the Ilulissat Ice Fjord mouth, west Greenland. *Quaternary Science Reviews*, *40*, 78–88. doi:doi:10.1016/j.quascirev.2012.02.016.

Seidenkrantz, M.-S., Aagaard-Sørensen, S., Sulsbrück, H., Kuijpers, A., Jensen, K., & Kunzendorf, H. (2007). Hydrography and climate of the last 4400 years in a SW Greenland fjord: implications for Labrador Sea palaeoceanography. *The Holocene*, *17*, 387–401. doi:10.1177/0959683607075840.

Seidenkrantz, M.-S., Ebbesen, H., Aagaard-Sørensen, S., Moros, M., Lloyd, J., Olsen, J., Knudsen, M., & Kuijpers, A. (2013). Early Holocene large-scale meltwater discharge from Greenland documented by foraminifera and sediment parameters. *Palaeogeography, Palaeoclimatology, Palaeoecology*, *391*, 71–81. doi:10.1016/j.palaeo.2012.04.006.

Seramur, K. C., Powell, R. D., & Carlson, P. R. (1997). Evaluation of conditions along the grounding line of temperate marine glaciers: an example from Muir Inlet, Glacier Bay, Alaska. *Marine Geology*, *140*, 307–27. doi:10.1016/S0025-3227(97)00026-1.

Sexton, D. J., Dowdeswell, J. A., Solheim, A., & Elverhøi, A. (1992). Seismic architecture and sedimentation in northwest Spitsbergen fjords. *Marine Geology*, *103*, 53–68. doi:10.1016/0025-3227(92)90008-6.

Shanmugam, G., Lehtonen, L., Straume, T., Syvertsen, S., Hodgkinson, R., & Skibeli, M. (1994). Slump and debris-flow dominated upper slope facies in the

Cretaceous of the Norwegian and northern North Seas (61-67 N): Implications for sand distribution. *AAPG bulletin*, *78*, 910–37.

Sheldon, C., Jennings, A., Andrews, J., Ó Cofaigh, C., Hogan, K., Dowdeswell, J., & Seidenkrantz, M.-S. (2016). Ice stream retreat following the LGM and onset of the west Greenland current in Uummannaq Trough, west Greenland. *Quaternary Science Reviews*, *147*, 27–46. doi:10.1016/j.quascirev.2016.01.019.

Smith, L. M., & Andrews, J. T. (2000). Sediment characteristics in iceberg dominated fjords, Kangerlussuaq region, East Greenland. *Sedimentary Geology*, *130*, 11–25. doi:10.1016/S0037-0738(99)00088-3.

Steenfelt, A., Thorning, L., & Tukiainen, T. (1990). *Regional compilations of geoscience data from the Nuuk-Maniitsoq area, southern West Greenland*. Grønlands Geologiske Undersøgelser.

Stewart, F., & Stoker, M. (1990). Problems Associated with Seismic Facies Analysis of Diamicton-Dominated, Shelf Glacigenic Sequences. *Geo-Marine Letters*, *10*, 151–6. doi:10.1007/BF02085930.

Stokes, C., Spagnolo, M., & Clark, C. (2011). The composition and internal structure of drumlins: complexity, commonality, and implications for a unifying theory of their formation. *Earth-Science Reviews*, *107*, 398–422. doi:doi:10.1016/j.earscirev.2011.05.001.

Streuff, K., Forwick, M., Szczuciński, W., Andreassen, K., & Ó Cofaigh, C. (2015). Landform assemblages in inner Kongsfjorden, Svalbard: evidence of recent glacial (surge) activity. *Arktos*, *1*. doi:10.1007/s41063-015-0003-y.

Stuiver, M., & Reimer, P. (1993). Extended ^{14}c data base and revised Calib 3.0 ^{14}c age calibration program. *Radiocarbon*, . doi:10.1017/S0033822200013904.

Syvitski, J., Andrews, J., & Dowdeswell, J. (1996). Sediment deposition in an iceberg-dominated glacimarine environment, East Greenland: basin fill implications. *Global and Planetary Change*, *12*, 251–70. doi:10.1016/0921-8181(95)00023-2.

Syvitski, J., & Murray, J. (1981). Particle interaction in fjord-suspended sediment. *Marine Geology*, *39*, 215–42. doi:10.1016/0025-3227(81)90073-6.

Vorren, T. O., Hald, M., Edvardsen, M., & Lind-Hansen, O. W. (1983). Glacigenic sediments and sedimentary environments on continental shelves: general principles with a case study from the Norwegian shelf. *Glacial Deposits in North-West Europe. Balkema, Rotterdam*, (pp. 61–73).

Walder, J., & Hallet, B. (1979). Geometry of former subglacial water channels and cavities. *Journal of Glaciology*, *23*, 335–46. doi:10.3198/1979JoG23-89-335-346.

Weidick, A. (1968). Observations on some Holocene glacier fluctuations in West Greenland. *Meddelelser on Grønland*, *165*, 202.

Weidick, A. (1994). Historical fluctuations of calving glaciers in south and West Greenland. *Rapport Grønlands Geologiske Undersølgelse*, *161*, 73–9.

Weidick, A. (1996). The Paleo-Eskimo Cultures of Greenland. New Perspectives in Greenlandic Archaeology. chapter Neoglacial changes of ice cover and sea level in Greenland–a classical enigma. (pp. 257–70). Danish Polar Center, Copenhagen.

Weidick, A., & Bennike, O. (2007). Quaternary glaciation history and glaciology of Jakobshavn Isbræ and the Disko Bugt region, West Greenland: a review. *Geological Survey of Denmark and Greenland Bulletin*, *14*, 13.

Young, N., Briner, J., Axford, Y., Csatho, B., Babonis, G., Rood, D., & Finkel, R. (2011a). Response of a marine-terminating Greenland outlet glacier to abrupt cooling 8200 and 9300 years ago. *Geophysical Research Letters*, *38*. doi:10.1029/2011GL049639.

Young, N., Briner, J., Rood, D., Finkel, R., Corbett, L., & Bierman, P. (2013). Age of the Fjord Stade moraines in the Disko Bugt region, western Greenland, and the 9.3 and 8.2 ka cooling events. *Quaternary Science Reviews*, *60*, 76–90. doi:10.1016/j.quascirev.2012.09.028.

Young, N., Briner, J., Stewart, H., Axford, Y., Csatho, B., Rood, D., & Finkel, R. (2011b). Response of Jakobshavn isbræ, Greenland, to Holocene climate change. *Geology*, *39*, 131–4. doi:10.1130/G31399.1.